Master's thesis

NTNU
Norwegian University of Science and Technology
Faculty of Medicine and Health Sciences
Kavli Institute for Systems Neuroscience

Jin Wang

A longitudinal EEG study of visual motion perception in full-term and preterm infants and children

Master's thesis in Neuroscience
Supervisor: Audrey van der Meer
May 2024

NTNU
Norwegian University of
Science and Technology

Jin Wang

A longitudinal EEG study of visual motion perception in full-term and preterm infants and children

Master's thesis in Neuroscience
Supervisor: Audrey van der Meer
May 2024

Norwegian University of Science and Technology
Faculty of Medicine and Health Sciences
Kavli Institute for Systems Neuroscience

NTNU
Norwegian University of
Science and Technology

Abstract

High-density electroencephalogram (EEG) was utilized longitudinally to study brain electrical activity in 10 full-term and 10 preterm participants at 4 months, 12 months, and 6 years of age, by investigating visual motion perception responses to structured optic flow and random visual motion. Analyses of visual evoked potentials (VEPs), temporal spectral evolution (TSE), and coherence connectivity were performed on EEG data recorded with 128/256-channel arrays. VEP results revealed significant improvements in full-term infants' latencies at 12 months for forwards and reversed optic flow, and at 6 years for random visual motion. Preterm infants did not show increased sensitivity to visual motion during the first year of life. However, at 6 years of age, preterm children reduced their N2 latencies to the level of the full-term children. At 12 months, full-term infants differentiated between visual motion conditions, with increased latencies observed from forwards optic flow to reversed optic flow and the longest latencies displayed for random visual motion. Preterm participants, on the other hand, did not demonstrate improved differentiation between visual motion conditions at either 12 months or 6 years of age. Analysis of N2 peak amplitudes exhibited significantly higher values in response to structured optic flow compared to random visual motion for both full-term and preterm participants at all ages. Moreover, a significant age-related decline in amplitudes for visual motion was observed between 12 months and 6 years for both full-term and preterm participants. Differences in induced activities were noted in comparisons between TSEs of visual motion and static control condition, revealing desynchronized activities predominantly in the theta-band range for infants at 4 months, transitioning to the theta-alpha band range when they were 12 months, and further extending into the alpha and beta ranges when they were tested at 6 years of age. Synchronized alpha-beta band activities were observed only in full-term infants at 12 months, while synchronizations at higher frequencies were noted in the beta and early gamma band ranges in 6-year-olds, especially in full-term children. Coherence connectivity analysis demonstrated greater functional connectivity within occipital and parietal areas in full-term participants compared to their preterm peers when comparing visual motion to static control condition. Specifically, only full-term children at 6 years of age displayed interactions with the PM source. Overall, divergent developmental trajectories were evident between full-term and preterm individuals from infancy to early childhood. Progression in visual motion perception for full-term participants during the first year of life to school age can be attributed to neural maturation and the formation of specialized networks. In contrast, the observed neurodevelopmental delay in preterm infants that persisted into school age was potentially linked to their premature birth resulting in an impaired dorsal visual processing stream.

Acknowledgement

I am deeply grateful for being given the opportunity to carry out my Master's thesis at the Developmental Neuroscience Laboratory (NuLab) at the Norwegian University of Science and Technology (NTNU) in Trondheim.

Firstly, I would like to express my deepest gratitude to my supervisor, Prof. Audrey van der Meer, for her invaluable guidance, support, and encouragement throughout the process of the work on my thesis. I am also deeply thankful to Seth Agyei and Silje-Adelen S. Nenseth, for answering all my questions and providing technical assistance, which greatly enriched the quality of this study. Thanks to my dear lab-mates for the great working environment, enjoyable conversations and evenings spent researching together.

Special thanks to Joe, who has consistently stood by my side, encouraging my continuous learning and independence, and to Zala and Wu, whose companionship has brought immeasurable joy and comfort throughout this journey. I am indebted to my family for the unwavering love, understanding, and encouragement, which sustained me through the highs and lows of my study at NTNU.

Finally, I extend my heartfelt appreciation to all the participants and their parents whose involvement made this study possible.

Gjøvik, May 2024

Jin Wang

Table of Contents

List of Figures

List of Tables

List of Abbreviations

BESA	Brain Electrical Source Analysis
dMST	dorsal Medial Superior Temporal Area
DEHSI	Diffuse and Excessive High Signal Intensity
DHA	Docosahexaenoic Acid
DTI	Diffusion Tensor Imaging
EEG	Electroencephalogram
ERD	Event-related Desynchronization
ERP	Event-related Potential
ERS	Event-related Synchronization
IT	Inferior Temporal Cortex
LGN	Lateral Geniculate Nucleus
MRI	Magnetic Resonance Imaging
MST	Medial Superior Temporal Area
MT	Middle Temporal Area
MT+	Middle Temporal Complex
M-ABC	Movement Assessment Battery for Children
NTNU	Norwegian University of Science and Technology
NuLab	Developmental Neuroscience Laboratory
PM	Parietal Midline
PPC	Posterior Parietal Cortex
SD	Standard Deviation
TEO	Posterior Portion of Inferior Temporal Area
TSE	Temporal Spectral Evolution
V1	Primary Visual Area
VCbL	Visual Cortex bilateral Left
VCbR	Visual Cortex bilateral Right
VClL	Visual Cortex lateral Left
VClR	Visual Cortex lateral Right
VCrL	Visual Cortex radial Left
VCrR	Visual Cortex radial Right
VCvM	Visual Cortex vertical Midline
VEP	Visual Evoked Potential

1 Introduction

1.1 Optic flow

Optic flow describes the systematic pattern of visual motion information perceived on the retina as an observer moves through or rotates within their environment (Gibson, 2014). It can be decomposed into a combination of vector fields including radial expansion or contraction, rotation, horizontal and vertical translation, and deformation of objects relative to an optically static point, corresponding to the observer's direction of movement (Koenderink, 1986). For instance, when moving forward, objects in the visual field appear to expand outward and a stream of light radiates out from the center. On the other hand, when moving backwards, the same objects appear to contract inward toward the central point and the flow radiates towards it (Bruce et al., 2003). This continuous perspective transformation of the light reflected from objects in the environment to the point of observation constitutes the dynamic pattern known as optic flow (Niehorster, 2021).

Optic flow is a fundamental aspect of visual perception during locomotion, which provides crucial information for understanding self-motion, perceiving spatial orientation, and navigating the environment (Gibson, 1950). It enables organisms to make rapid and accurate judgments about their movements and spatial relationships with surrounding objects, thereby enhancing the adaptive capabilities of the visual system in dynamic contexts (Browning et al., 2009; Gibson, 1950). It significantly contributes to behavior, furnishing cues for walking (Warren et al., 2001). Optic flow plays a vital role in the perception of one’s own motion and depth, computing heading, or direction of travel, and facilitating path integration during navigation (Kirschen et al., 2000; Warren & Hannon, 1988).

1.2 Visual motion perception

Most daily activities depend on perceiving and correctly interpreting visual information from the environment, which also plays an essential and important role for survival in a dynamic visual world (Albright & Stoner, 1995). The ability of the visual system to detect and integrate motion information in the environment is termed visual motion perception. Visual motion perception encompasses various types of motion, self-motion, object motion, and biological motion, each contributing to our understanding of movement and spatial relationships within the visual environment (Blake & Shiffrar, 2007; Gupta et al., 2009; Lappe et al., 1999). It enables everyday functions of self-motion, perceiving time-to-contact (Kayed & Van der Meer, 2009) and avoiding obstacles (Fajen & Matthis, 2013; Wilkie & Wann, 2003), orientation and heading direction (Grossberg et al., 1999), control of posture (Vaina & Rushton, 2000), and efficient locomotion and navigation (Borge Blystad & Van der Meer, 2022; Lappe et al., 1999).

Visual motion, generated by both self-motion and objects moving within the visual field, is detected as optic flow (Kleinschmidt et al., 2002). The relation between perception of optic flow and action is crucial for motor functions and has been extensively studied in the context of motor activities. Research using brain and behavioral data has revealed that infants perceive optic flow to provide information for prospective control, guiding

hand-reaching actions to intercept moving objects during early infancy, while also facilitating anticipatory adjustments in movement thereafter (Agyei et al., 2016b). Behavioral experiments have demonstrated that perception of optic flow influences the control of walking speed and direction (Bruggeman & Warren, 2010; Lalonde-Parsi & Lamontagne, 2015; Lamontagne et al., 2007; Vilhelmsen et al., 2015; Warren et al., 2001). Locomotor tasks in virtual environments have shown that perceiving both visual and non-visual information from optic flow enhances accuracy in perceiving object motion (Fajen & Matthis, 2013). Furthermore, the effective estimation of speed and calibration of action for navigation relies on integrating visual speed derived from optic flow with speed gauged from proprioceptive and locomotor systems (Mohler et al., 2004; Saleem et al., 2013).

1.3 Development of visual perception of optic flow pattern

Observing others perform an action can aid in acquiring new motor skills, while motor learning processes improving visual perception through action-to-perception transfer has been reported in adults (Beets et al., 2010). However, young infants do not have all the action systems for motor processes (Gibson, 2014), hence the ability to detect optic flow may not be as effective as in adults (Gilmore et al., 2007; Van der Meer et al., 2008). Understanding the developmental processes through which infants use relevant visual information for perception is crucial for uncovering the neural mechanisms of visual motion perception and promoting healthy development.

The rudimentary perception of optic flow patterns emerges within the first weeks and months after birth (Gilmore et al., 2004). Infants younger than one month exhibit avoidant responses, such as avoidant head leaning, backward body motion, and blinking, when exposed to radial expansion flow (Shirai & Imura, 2014; Shirai & Yamaguchi, 2010; Yonas, 1981). In addition, neonates as young as three days old respond with backward leaning of the head to bilateral and backward peripheral optic motion (Jouen et al., 2000). However, these defensive motor responses have been interpreted as the result of multimodal integrative and cooperative processes involving visual, vestibular, and proprioceptive senses, rather than being a direct consequence of motion perception (Guitton et al., 1986; Jouen et al., 2000).

Further behavioral and electroencephalogram (EEG) studies have revealed developmental milestones in infants' visual motion perception, showing variation in perceptual development across different types of optic flow patterns, including translation, rotation, and radial expansion or contraction. At approximately 2 months of age, the ability to discriminate translational motion patterns emerges: infants younger than 6-8 weeks of age do not discriminate motion direction and are not capable of following small moving objects with smooth pursuit, whereas between 6 and 14 weeks of age, these abilities rapidly improved (Braddick et al., 2005; Rosander et al., 2007). By two to three months of age, infants remain insensitive to rotation (Shirai et al., 2008), but demonstrate discrimination of optic flow patterns simulating large changes in heading direction as early as 3 months of age (Gilmore et al., 2004). Additionally, infants show enhanced sensitivity to expanding radial motion during the first months of life (Brosseau-Lachaine et al., 2008). However, the development of radial motion perception and its cortical responses in infancy is often reported to be severely limited at 2 months, while showing rapid development at 3-4 months of age (Gilmore et al., 2007; Shirai & Yamaguchi, 2010). Furthermore, at 4-6 months, infants show evoked brain activity to distinguish radial motion to translation or rotation from optic flow patterns (Gilmore et al., 2007).

Moreover, infants' preference for contraction flow significantly diminishes one month before the onset of locomotor which increased between 7 and 8 months (Brosseau-Lachaine et al., 2008; Shirai & Imura, 2014). A developmental plateau in radial motion perception has also been noted after the first few months and perceptual development remains immature until at least 8 months of age (Gilmore et al., 2004; Shirai & Imura, 2014). This suggests that the perception of optic flow and locomotion ability develop separately during earlier developmental stages and become interconnected in later stages, perhaps through experiences of self-generated locomotion (Shirai & Imura, 2014).

Visual motion perception gradually improves throughout childhood and adolescence, reaches maturity, yet continues to undergo fine-tuning throughout the transition to adulthood (Bogfjellmo et al., 2014; Gilmore et al., 2016; Joshi & Falkenberg, 2015). Adult-level performance is likely not attained before approximately 4 years of age (Agyei et al., 2016a; Kaufmann, 1995; Parrish et al., 2005) and adult-like pattern of neural responses to optic flow begins to emerge by early to middle childhood (Gilmore et al., 2016). Studies have shown that sensitivity to translational optic flow approaches adult-like levels by 6-14 years of age, depending on the stimulus parameters and task complexity (Joshi & Falkenberg, 2015). Perception of radial optic flow gradually develops but matures later compared to translational flow (Joshi & Falkenberg, 2015). Perception of radial flow undergoes development between 6-12 years of age but is not fully developed (Izumi et al., 2017; Rasulo et al., 2021), as evidenced by the continued immaturity in discriminating radial optic flow patterns even at 16 years of age (Joshi & Falkenberg, 2015). Perceptual sensitivity to complex optic flow patterns, like expansion and rotation, develops later in childhood (Baumberger & Flückiger, 2004).

1.4 Neural bases of visual motion perception

Various brain studies in humans and other primates have investigated the neural mechanisms involved in visual motion perception. Incoming light is transduced into neural signals by the retina, which passes information to the lateral geniculate nucleus (LGN), and then to primary visual area (V1) in cortex and higher visual areas (Johnson, 2011). The idea of a division between two separate yet heavily interconnected streams, a ventral and a dorsal visual stream, is one of the most basic principles of processing visual information (Milner & Goodale, 2006). The ventral stream originates from V1 through V2, V3, and V4, and the posterior portion of inferior temporal area (TEO) to inferior temporal cortex (IT), while the dorsal stream arises from V1 through V2, V3, middle temporal area (MT), medial superior temporal area (MST) to the posterior parietal cortex (PPC) (Creem & Proffitt, 2001). Referred to as the "what" pathway, the ventral stream is critical for object recognition and stimulus identification, whereas the dorsal stream, or "where" and "how" pathway has been primarily associated with visually guided movements, visuomotor control, and spatial perception (Agyei et al., 2016a; Gallivan & Goodale, 2018; Hebart & Hesselmann, 2012; Milner & Goodale, 2006; Rizzolatti & Matelli, 2003).

The brain area termed MT/V5+ includes the middle temporal visual area MT/V5 along with adjacent motion-sensitive areas such as MST (He et al.,1998). Located within the occipital and temporal lobes, MT/V5+ is widely recognized for its specialization in processing motion information, particularly in perception and interpretation of optic flow, encompassing object movement and self-motion through the environment (Born & Bradley, 2005; Giaschi et al., 2007; Layton & Fajen, 2016; Morrone et al., 2000; Newsome & Pare, 1988; Tootell et al., 1995). While both MT and MST are implicated in

the processing of translational motion (Giaschi et al., 2007; Ortibus et al., 2011), it appears only neurons in the dorsal medial superior temporal (dMST) area makes a causal contribution to the perception of radial motion (Duffy & Wurtz, 1991; Smith et al., 2006; Strong et al., 2017). Additionally, neural activation in dMST varies with specific combinations of optic flow components (Duffy & Wurtz, 1991; Grossberg et al., 1999; Smith et al., 2006; Zemel & Sejnowski, 1998).

The human brain forms a dynamic, organized network of interconnected neurons and synapses, enabling remarkable plasticity, which is obvious in both the visual cortex and associated functions (Hensch, 2005). The period of time in an individual's ontogeny when the plasticity of neuronal circuits is enhanced and certain functions or abilities must be adequately stimulated, or they risk being impaired or lost, are termed critical periods (Johnson, 2011; Levelt & Hübener, 2012). The plasticity of visual cortex and visual functions might vary in their developmental timing (Hensch, 2005), presenting well before, and long after, the peak of the critical period (Levelt & Hübener, 2012). The understanding of the neural basis for brain development and plasticity has been strengthened with advances in neuroscience. Studies have revealed that visual cortex development including myelination of axons, increases in dendritic length, cortical thinning and GABAergic signaling mechanisms, occurs during critical periods after birth, and continues to develop even after the first decade of life (Joshi & Falkenberg, 2015; Kolb & Whishaw, 1998). These anatomical changes are correlated with behavioral differences between individuals (Kolb & Whishaw, 1998) and extensive learning from experience (Johnson, 2011). Based upon the type of information stored and the involved brain mechanisms, Greenough and colleagues introduced the term "experience-expectant plasticity" to describe the influence on developing and mature brains by ubiquitous experience (Greenough et al., 1987). It likely underlies sensitive or critical period phenomena, with neural mechanisms leveraging certain experiences consistently provided by the normal environment to prune and shape the intrinsic generation of an excess of synaptic connections, thereby evolving the sensory and motor systems (Greenough et al., 1987; Jones & Jefferson, 2011). For instance, the onset of and increase in locomotor experience may prune overproduced cortico-cortical synaptic connections between frontal/occipital and parietal/occipital sites (Bell & Fox, 1996) and form specialized neural networks for rapid processing of various visual and motor information (Borge Blystad & Van der Meer, 2022). Premature and low-birth-weight infants are at high risk for neurodevelopmental abnormalities and visual impairments (Bonnier, 2008; Ortibus et al., 2011; Perez-Roche et al., 2016). Considering that profound plasticity of the visual system occurs during early life (Bonnier, 2008; Takesian & Hensch, 2013), it is important to investigate how an interplay of life experience and maturation may impact the visual plasticity and functional development of premature infants.

1.5 Visual motion perception of preterm individuals

The World Health Organization defines preterm birth as any birth before 37 completed weeks of gestation, and this can be subdivided into extremely preterm (<28 weeks), very preterm (28-31 weeks), moderate preterm (32-33 weeks), and late preterm (34-36 weeks) (Ohuma et al., 2023). The global preterm prevalence was around 10% over the past decade (Ohuma et al., 2023). With the survival rate of preterm infants improved by advanced medical care, the impact of premature birth on later visual and visuocognitive development received more attention. Magnetic resonance imaging (MRI) and diffusion tensor imaging (DTI) studies have identified abnormalities in tissue microstructure and

cerebral morphology among preterm individuals at different ages (Counsell & Boardman, 2005). In particular, preterm individuals exhibiting visuomotor deficits show structural alterations in several specific gray-white matter networks and reduced surface area of motor and visual cortices (Sripada et al., 2015). Studies spanning different developmental stages from infancy to adulthood have reported deficits in visual perceptual and visuomotor skills over the long term among preterm individuals (Guzzetta et al., 2009; Leung et al., 2018; Molloy et al., 2013; Ortibus et al., 2011; Pel et al., 2016; Sripada et al., 2015). Additionally, apparently healthy preterm infants may suffer some degree of loss of neurological function (Madan et al., 2005). Behavioral experiments have shed more light on deficits in motion perception among preterm children, where preterm children without brain damage show poor accuracy and sensitivity in both rotation and linear translation optic flow perception but have similar performance in form perception compared to age-matched, full-term peers; however, those with brain damage perform worse on both motion and form perception (Benassi et al., 2018; Guzzetta et al., 2009). These observations suggest the dorsal pathway is particularly vulnerable to prematurity per se as motion perception is impaired in all preterm children regardless of the presence or absence of brain damage (Guzzetta et al., 2009). Further studies utilizing multiple assessment techniques have pointed out that the cluster of deficits observed in prematurely born children may be linked to impairment of the visual dorsal stream and its connections to parietal, frontal, and hippocampal areas (Atkinson & Braddick, 2007). These findings are reinforced by other studies comparing global motion, global form, and biological motion (combination of cues for form and motion) perception in preterm children (e.g., Taylor et al., 2009).

Interestingly, several studies support the notion that preterm infants benefit from early exposure to an extrauterine environment, which accelerates the development of visual abilities as a result of additional experience (Hunnius et al., 2008; Madan et al., 2005). Electrophysiological techniques in preterm infants have demonstrated accelerated maturation of the visual evoked potential (VEP) and visual cortex, whereas myelination of the optic radiation and white matter tracts remain unaffected (Madan et al., 2005). Given that previous studies in preterm infants have included a broad range of gestational ages and that a collection of preterm infants represents a heterogeneous group, it is necessary to understand the developmental patterns of individuals born prematurely at various degrees of prematurity across different ages.

1.6 EEG studies in visual motion perception

EEG has become indispensable in experimental studies of human brain function (Michel, 2019), due to its non-invasive nature and high temporal resolution at the millisecond scale. Technology advancements have enabled high-density EEG to achieve source localization with higher spatial resolution of neural signals (Krishnan et al., 2018; Michel, 2019). This has been beneficial for psychophysiological research on visual motion perception, where EEG serves as a valuable tool for investigating visual evoked potentials, time-frequency activities, and the functional connectivity of networks.

The neuronal basis of motion perception and the functional specializations of cortical structures can be studied using EEG, which primarily records the electrical activities of large cortical pyramidal neurons in deep cortical layers because of their unique orientation with their long apical dendrites perpendicular to the cortical surface (Kirschstein & Köhling, 2009; Pfurtscheller & Da Silva, 1999). Various events, notably sensory stimuli, can induce time-locked changes in the activity of neuronal populations,

which is a type of evoked activity commonly referred to as event-related potentials (ERPs) (Pfurtscheller & Da Silva, 1999). VEP is a specific type of ERP elicited by visual stimuli (Odom et al., 2004). During visual processing, motion-sensitive VEP waveforms in EEG are dominated by a negativity (N2) which is typically observed from V5/MT+ in posterior occipital and parietal areas (Luck, 2014). Previous studies have indicated that infants show longer N2 latencies and larger amplitudes compared to adults (Van der Meer et al., 2008), with latencies decreasing with age (Agyei et al., 2015). In adults, the latency peak occurs around 130-200 ms post stimulus, while in infants aged 11-12 months, it occurs around 270-290 ms after onset of stimulus, and at 3-4 months around 330-430 ms (Agyei et al., 2015; 2016a; Heinrich et al., 2005; Kobayashi et al., 2004; Kuba & Kubová, 1992; Rasulo et al., 2021; Vilhelmsen et al., 2015; 2019). Similar results have been observed in studies of P1, N1, and P2 components, where latencies decrease with increasing age (Fielder et al., 1983; Hammarrenger et al., 2007). In addition, EEG studies from infancy through adulthood have consistently revealed that structured optic flow is processed more rapidly than random visual motion, especially after the onset of self-generated locomotion (Agyei et al., 2015; 2016a; Borge Blystad & Van der Meer, 2022; Van der Meer et al., 2008). However, the differentiation between structured optic flow and random visual motion with self-generated locomotion was observed only in full-term infants, and this tendency has not been observed in preterm-born infants (Agyei et al., 2015; 2016a; Borge Blystad & Van der Meer, 2022).

In addition to the VEPs in EEG studies, a growing number of researchers have been investigating the time-frequency domain, which allows computing the temporal dynamics of EEG oscillations with a technique called temporal spectral evolution (TSE). EEG recordings can be categorized as ongoing, evoked, or induced oscillations (David et al., 2006). Given that evoked activity is both time- and phase-locked to the stimulus, while the ongoing EEG oscillations act as additive noise, averaging procedure can enhance the signal-to-noise ratio (Pfurtscheller & Da Silva, 1999). In contrast, induced activity refers to rhythmic neural oscillations that emerge in response to cognitive processes which are not phase-locked to the stimulus and are revealed by spectral analysis (David et al., 2006). TSE enables the extraction of event-related frequency changes in EEG that cannot be observed in VEPs through averaging techniques (Agyei et al., 2016a). Modulations of oscillatory activity can be observed as event-related synchronization (ERS) or event-related desynchronization (ERD), indicating an increase or decrease in power or amplitude within specific frequency bands (Pfurtscheller & Da Silva, 1999). This serves as an indication of changes in synchrony among the underlying neuronal populations (Pfurtscheller & Da Silva, 1999). Different classes of oscillations have been distinguished over the years: delta-band (1-4 Hz), theta-band (4-7 Hz), alpha-band (7-13 Hz), beta-band (13-30 Hz), and gamma-band (30-150 Hz) (Buzsaki & Draguhn, 2004; Ganzetti & Mantini, 2013). These oscillations reflect neurophysiological processes that are functionally relevant to distinct roles (Buzsaki & Draguhn, 2004; Pfurtscheller & Da Silva, 1999). For example, delta-band oscillations are associated with deep sleep stages, but they can also be observed during cognitive tasks related to signal detection and decision making (Başar et al., 2001). Event-related alpha ERS plays an active role for inhibitory control and ERD reflects the gradual release of inhibition (Klimesch et al., 2007). Different types of theta amplitude modulations subserve a variety of cognitive processes including sustained attention and working memory maintenance (Freunberger et al., 2011; Kahana et al., 2001).

A strong increase of power in the gamma-band (Hoogenboom et al., 2006), an induced increase in beta-band (Van der Meer et al., 2008; Vilhelmsen et al., 2019), and alpha-

band ERD and ERS (Pfurtscheller et al., 1994; Vilhelmsen et al., 2015) in response to visual stimulation have been reported in adults. The high-frequency activation in adults reflects a fully developed motion perception system (Van der Meer et al., 2008; Vilhelmsen et al., 2019). Further EEG studies using optic flow and TSE analysis in infants and children have reported induced desynchronized oscillatory activity in theta and alpha bands for infants (Van der Meer et al., 2008; Vilhelmsen et al., 2019), and desynchronized oscillatory activity in the alpha and beta bands for children (Rasulo et al., 2021). In particular, desynchronized theta-band activity is observed in both full-term and preterm infants at 4 and 12 months, while synchronized alpha-band activity is observed only in full-term infants at 12 months (Agyei et al., 2015; 2016a). Additionally, synchronized beta-band activity is observed in full-term infants with swimming experience at both 4 months and around 12 months (Borge Blystad & Van der Meer, 2022). The increase in frequency band and ERS with age and locomotor experience suggests a progression of specialized and effective neuronal networks toward a more mature form of visual motion perception. This progression is supported by the transition of EEG spectral amplitudes from lower to higher frequencies, which is considered a marker of maturation during development of cortical function and neural networks (Hudspeth & Pribram, 1992).

There is a growing interest in source modeling to investigate interactions between functionally specialized brain regions (Schoffelen & Gross, 2009; Xie et al., 2022). High-density EEG is a technique suited to capture these interactions, particularly when dealing with pediatric populations, because it can overcome the effects of volume conductance and provide whole head measurements of brain activity noninvasively in the millisecond range (Barzegaran & Knyazeva, 2017; Schoffelen & Gross, 2009; Xie et al., 2022). The EEG functional connectivity is typically estimated by analyzing the correlation or coherence through brain sources reconstructed from scalp signals, which has been evaluated and used in many studies (Hassan et al., 2014; Miskovic et al., 2015; Schoffelen & Gross, 2009; Xie et al., 2022). Brain functional connectivity in children exhibits distinct patterns across frequency bands and changes with age, possibly indicating the pruning of connections during development (Xie et al., 2022). Additionally, connectivity differences have also been identified between healthy elderly individuals and mild cognitive impairment patients potentially aiding in the clinical diagnosis of dementia (Gómez-Herrero, 2010). However, there is limited information regarding the accurate identification of interactions between brain regions in source space related to visual perception from EEG data.

1.7 The present study

The present study aimed to investigate the development of visuo-cognitive systems, specifically focusing on visual motion perception from early infancy to childhood, utilizing high-density EEG. The objective was to shed light on the typical development of visual motion perception and potential developmental impairments linked to motion perception in preterm infants and children. By leveraging EEG longitudinal data, this study compared full-term and preterm infants and children at 4 months, 12 months, and 6 years of age using a combination of VEPs, time-frequency oscillations (TSE), and coherence connectivity analyses. It was hypothesized that visual motion perception would exhibit rapid improvement with age, particularly in full-term infants, characterized by the shortest latencies and lowest amplitudes for forwards optic flow, followed by reversed optic flow, with no notable enhancement in the perception of random visual motion expected. An induced decrease in amplitude in low frequencies was anticipated in infants,

accompanied with a shift from low- to high-frequency desynchronized oscillatory brain activity in response to visual motion as age increased. Moreover, synchronized oscillatory activities in high frequency bands were expected to be more pronounced in older infants and children. Additionally, disparities in motor performance and connectivity networks in the visual areas were anticipated between full-term and preterm participants from late infancy to childhood. Based on previous research in preterm infants, indicating impaired dorsal stream functionality, it was predicted that they would display delayed development of visual motion processing during the first year of life compared to their peers. However, they might catch up with full-term children by the age of 6 years.

2 Method

2.1 Participants

A total of 20 normally developing infants, 10 full-term (5 boys and 5 girls) and 10 preterm (4 boys and 6 girls), were recruited for the longitudinal study. The full-term infants were recruited by contacting parents via birth announcements, while the preterm infants were recruited through the Neonatal Intensive Care Unit at St. Olav's University Hospital in Trondheim. The full-term infants had a mean gestational age of 40.7 weeks (SD=1.1, median=40.7, range=39.0-41.9) and mean birth weight of 3607 g (SD=576, median=3450, range=3085-5120). The preterm infants (moderate to very preterm) were born at a mean gestational age of 31.2 weeks (SD=2.3, median=32.5, range=26.1-33.0), with a mean birth weight of 1609 g (SD=543, median=1635, range=710-2670). The preterm infants had no major neurological deficits including severe brain damage, retinopathy of prematurity (ROP), and were devoid of other perinatal issues requiring serious medical interventions that could lead to abnormal development, but only one girl suffered a brain hemorrhage (grade 3) during her first week of life.

Infants were tested at 4 months and 12 months, followed by a third testing during early childhood at 6 years of age, using a longitudinal design. For the first testing session, the mean age of the full-term infants was 4 months and 9 days (SD=20) with a range of 105-163 days, and the mean age of the preterm infants was 4 months and 25 days (SD=6) with a range of 136-156 days. None of the infants had experience with self-locomotion at the first testing session. For the second testing session, the mean age was 11 months and 16 days (SD=16) with range 314-366 days for full-term infants, and 12 months and 4 days (SD=18) with range 338-407 days for the preterm infants. By this point, all infants could crawl, and some of them could independently pull to stand, walk alone, or walk with help, except for two preterm infants who were bottom shuffling instead (parental report). For the third testing session, the mean age of the full-term children was 6 years and 7 months (SD=7) with a range of 66-87 months, and the mean age of the preterm children was 6 months and 2 months (SD=9) with a range of 60-81 months. At this age, all the children had started primary school. Preterm ages were corrected for prematurity.

Electroencephalography is a non-invasive physiological procedure with no known harmful or painful effects on participants. Prior to the experiment, parents provided informed written consent and had the right to withdraw from the testing at any time before or during the experiments. The study received approval from the Norwegian Regional Ethics Committee and the Norwegian Data Services for the Social Sciences. All testing for the study took place at the Developmental Neuroscience Laboratory (NuLab) within the Department of Psychology at the Norwegian University of Science and Technology (NTNU) in Trondheim, Norway.

2.2 Experimental stimuli and paradigm

Stimuli were generated with E-prime software (Psychological Software Tool) and mirror-projected onto a wide screen (108 cm wide, 70 cm high) by means of an ASK M2 projector with a refresh rate of 60 Hz. Participants were seated approximately 70 cm

from the screen, ensuring that the angles subtended by the width and height of the screen were 68.0° and 46.7°, respectively. Stimuli consisted of 100 black randomly placed dots on a white background, each with a virtual radius of 5 mm. To discriminate between coherent and incoherent radial motion, three motion conditions were employed: forwards optic flow, reversed optic flow, and random motion. Duration of presentation for motion stimuli was 1500 ms, with the order randomly chosen. A static non-flow condition lasting 1500 ms after each motion pattern was included to suppress the effect of motion adaptation and served as baseline for the TSE analysis. A red fixation point, with a diameter of 1.69 mm, subtended an angle of 0.16° at the center of the screen. The size of dots varied gradually at a rate of 0.025 pixels per pixel as a function of their distance to the position of the reference fixation point, such that the dots appeared small when far from the eye and large when close in virtual space. In three motion conditions, dots moved towards and away from the screen's center at a constant rate of 30 mm per frame at a rate of 60 frames per second.

To simulate forwards optic flow, dots appeared to move coherently towards the participant. Movement was parallel to the z-axis towards the eye with velocities in the x- and y-axes remaining zero. For reversed optic flow, dots moved coherently in the opposite direction to that of forwards optic flow. All the dots moved parallel to the z-axis as in the forwards optic flow but away from the eye with velocities in the x- and y-axes also at zero. Unlike the above two conditions, the dots in the random motion condition moved in a completely random direction in virtual space at the same constant speed. The static control condition, which was a frozen optic flow condition, presented at the end of the preceding trial, had dots stay in the same position as long as the trial lasted. As in the motion conditions, dots in the static control condition had varying sizes on the screen, ranging from a 2 mm radius to 17 mm radius.

In the motion conditions, accretion of dots at the center or edges of the screen was avoided by presenting stimuli as a uniform dot distribution. Dots moving beyond the range of sight on the screen were automatically resized and repositioned on the screen with the same probability in each motion condition.

2.3 Data acquisition

EEG activity was recorded with a Geodesic Sensor Net 200 (GSN) consisting of an array of 128 sensors for infants and 256 sensors for children, evenly distributed over the scalp. A high-input EGI amplifier connected to the net ensured signal amplification with a maximum impedance of 50 kΩ as recommended for optimal signal-to-noise ratio (Budail et al., 1995; Ferree et al., 2001; Picton et al., 2000). Amplified EEG signals were recorded via Net Station software on a Macintosh computer at a sampling rate of 500 Hz. Concurrently, gaze was captured using an infrared Tobii X50 camera to ensure that the participants were looking at the screen. The visual feed was processed by ClearView software on an HP computer. Two additional digital cameras positioned at different angles in front of the participants recorded behavior during the experiment. All collected data was stored for further off-line analyses.

2.4 Procedure

Parents arrived at the lab with their infant or child some time before the experiment to sign the consent form. The infant or child was then allowed to acclimate to the laboratory surroundings by playing with toys and exploring the new environment. Participant’s head circumference was measured by an assistant to select the appropriate net for the

experiment. The net was soaked in a warm saline electrolyte to ensure good impedance and comfort, slightly dried with a towel, and mounted on the infant's or child's head while seated on the parent's lap or in a chair. To divert the infant's attention from the net, assistants blew soap bubbles and used small sounding toys. Immediately after the net was mounted, the infant or child was moved into a dimly lit experimental room which was separated from the control room by a transparent glass partition. Two assistants operated the computers required for data acquisition in the control room. The infant was seated on the parent's lap or in a baby car seat for the first testing session, in a baby car seat during the second testing session, and in an adjustable chair for the third testing session. An assistant sat nearby to help the infant or child focus on the screen and monitor the experiment, while a parent remained present in the experimental room throughout the sessions to alleviate any potential stress from their absence. The net was plugged into the amplifier after the participant was seated. Impedance was checked before the beginning of the experiment in the control room. If needed, the contact of electrodes was improved by adding additional saline solution to them or simply adjusting their position.

After the gaze was calibrated in virtual space, the experimental session began immediately. The session typically started with the optic flow experiment, followed by two other visual motion experiments. The optic flow experiment lasted 5 to 7 minutes, with each participant presented with 80 to 120 trials, half of which were static control trials. Data acquisition was carried out in one block, but when an infant or child showed signs of boredom or disinterest, the session was temporarily paused. During this break, the assistant and/or parent engaged with the infant or child to revive their interest before resuming the presentations. An experimental session concluded if the participant showed a considerable level of disinterest, fussiness, or tiredness.

2.5 Brain data analysis

EEG raw data were analyzed with Brain Electrical Source Analysis (BESA) Research software version 7.0, BESA Statistics 2.1 (BESA GmbH) and BESA Connectivity 2.0. The procedure was the same for all three testing sessions for both groups. Data analyses started with several pre-processing steps. EEG recordings were segmented using Net Station software and exported as raw files, with auxiliary files containing trigger and sensor information attached. Epochs of interest were set with averaging epochs from -200 ms to 800 ms with a baseline definition of -100 ms to 0 ms. The notch filter was set at 50 Hz to avoid line interference. The low cut-off filter was set at 1.6 Hz to remove slow drift in the data, and high cut-off filter was set at 60 Hz to remove channels contaminated with high-frequency activities. By visual inspection, artifact-contaminated channels and epochs resulting from head or body movements as well as instances where infants were not looking at the screen were excluded from further analyses, or the data interpolated manually where necessary. The maximum limit of channels defined as bad was set to 10%. Participants, with more than 10% of the channels defined as bad, were not included in the analyses. Physiological artifacts caused by blinking or eye movements were corrected manually or through a semi-automatic artifact correction designed to separate brain activities from artifacts using appropriate spatial filters (Berg & Scherg, 1994; Fujioka et al., 2011; Ille et al., 2002; Shao et al., 2008). In scanning for artifacts, threshold values for gradient and low signal were set at 75 μV and 0.1 μV, respectively, while maximum amplitude was set at 200-220 μV for infants, and 120-300 μV for children.

The mean numbers of accepted motion trials for full-term infants at 4 months, 12 months, and children at 6 years were 54 (SD=13.4), 44 (SD=22.8), and 49 (SD=13.6), respectively, while those for preterm participants were 47 (SD=22.3), 56 (SD=16.6), and 59 (SD=8.5), respectively. Accepted trial numbers were approximately evenly distributed across the three motion conditions in all testing sessions. For the static control condition, the average number of accepted trials contributed by full-term infants and children was 59 (SD=16.0) at 4 months, 46 (SD=24.1) at 12 months, and 50 (SD=13.0) at 6 years. The corresponding mean numbers of accepted trials for preterm infants and children were 48 (SD=23.1), 57 (SD=15.2), and 59 (SD=5.9) at 4 months, 12 months, and 6 years.

2.6 VEP peak analysis at the electrode level

Individual averages were obtained by exporting EEG data into the standardized 81-electrode configuration of the 10-10 International system after re-referencing to an artificial reference calculated from the average potentials over the scalp. The individual averages from each group and testing session were combined into grand averages. Grand average VEPs provided approximate time intervals that served as reference intervals for selecting individual N2 components across various electrode sites. The N2 components of the VEP waveforms were identified using 3D spherical spline whole-head voltage maps of EEG scalp signal distribution, aiding in visualizing maximum N2 activity in occipito-parietal areas for the most dominant waveform. Peak latencies were measured from stimulus onset to the peak of each N2 component. Values for both peak latencies and peak amplitudes of the individual averages were recorded for further analysis.

2.7 Time-frequency analysis in brain space

Time-frequency analysis, representing changes in amplitude over time (TSE, temporal spectral evolution) was performed in brain space using multiple pre-defined source dipoles that modelled activities in the main brain regions, including visual areas of the parietal and visual cortices. Using surface electrodes to measure brain oscillatory activities may not be ideal since scalp waveforms receive mixed contributions from underlying brain sources. This arises from the wide distribution of focal brain activity caused by the smearing effect of brain volume conduction in EEG and the nature of dipole fields. The optimal separation of focal brain activities can be achieved by using a source montage obtained via a multiple source model (Scherg & Berg, 1991; Scherg et al., 2002), wherein source waveforms are maximally separated activities from different brain regions. The source montage consisted of 17 sources modelling activities in the visual pathway as well as any residual activities in other regions of the brain (Figure 1). The regional sources of visual cortex bilateral left (VCbL), visual cortex lateral left (VClL), visual cortex radial left (VCrL), the parietal midline (PM), visual cortex vertical midline (VCvM), visual cortex radial right (VCrR), visual cortex lateral right (VClR), and visual cortex bilateral right (VCbR) that are believed to be active in the visual processing of motion stimuli (Probst et al., 1993; Van der Weel & Van der Meer, 2009; Zeki et al., 1991). Of these sources, VClL, VCrL, PM, VCvM, VCrR, and VClR were used for TSE analysis (Figure 2). To analyze brain activities using these sources, a 4-shell ellipsoidal head model (Berg & Scherg, 1994; Hoechstetter et al., 2004; Scherg et al., 2002) was created for each participant and the source dipoles were inserted while the artifact-corrected coordinate files were appended. As recommended, bone thickness was set to 3.0 mm and conductivity to 0.02 σ for infants, while for children, it was adjusted to 5.0 mm for bone thickness and 0.0 σ for conductivity (Grieve et al., 2003; BESA

information). The same settings for epoch, filter, and average parameters as used in the VEP analyses were maintained.

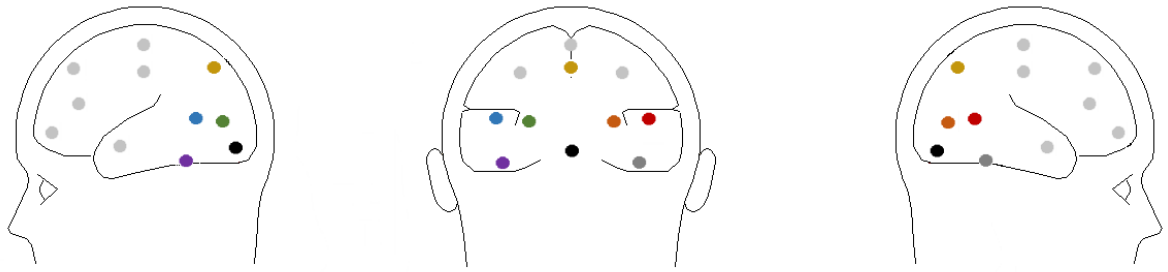

Figure 1: Head model with illustration of the 17 sources, with sources of interest: visual cortex bilateral left (VCbL), visual cortex lateral left (VClL), visual cortex radial left (VCrL), partietal midline (PM), visual cortex vertical midline (VCvM), visual cortex radial right (VCrR), visual cortex lateral right (VClR), and visual cortex bilateral right (VCbR). The approximate Talairach coordinates of the sources are x = -40.0, y = -48.6, z = -22.7 for VCbL; x = -45.2, y = -57.2, z = 6.5 for VClL; x = -25.6, y = -73.0, z = 4.2 for VCrL; x = 0.0, y = -72.3, z = 37.0 for PM; x= 0.0, y = -84.9, z = -14.3 for VCvM; x = 25.6, y = -73.0, z = 4.2 for VCrR; x = 45.2, y = -57.2, z = 6.5 for VClR; and x = 40.0, y = 48.6, z = -22.7 for VCbR (Talairach & Tournoux, 1988).

Time-frequency displays were generated from single trials by averaging spectral density amplitudes over trials. Each graph was a plot of spectral amplitude density of a single montage channel over time and frequency normalized to the baseline for each frequency. To focus only on induced oscillatory brain activity, average evoked response signals were removed from the single trial time series before computing a TSE. Independent TSEs for the three motion conditions (forwards optic flow, reversed optic flow, and random visual motion), comparisons between each of the motion conditions and the static control condition, as well as between the combined visual motion and the static control condition were computed. TSE displays for infants and children were configured with a frequency cut-off of 4-40 Hz, with frequency and time sampling set at 1 Hz and 50 ms, respectively. The frequency cut-off was further adjusted to explore oscillatory activities within both the delta and gamma frequency ranges.

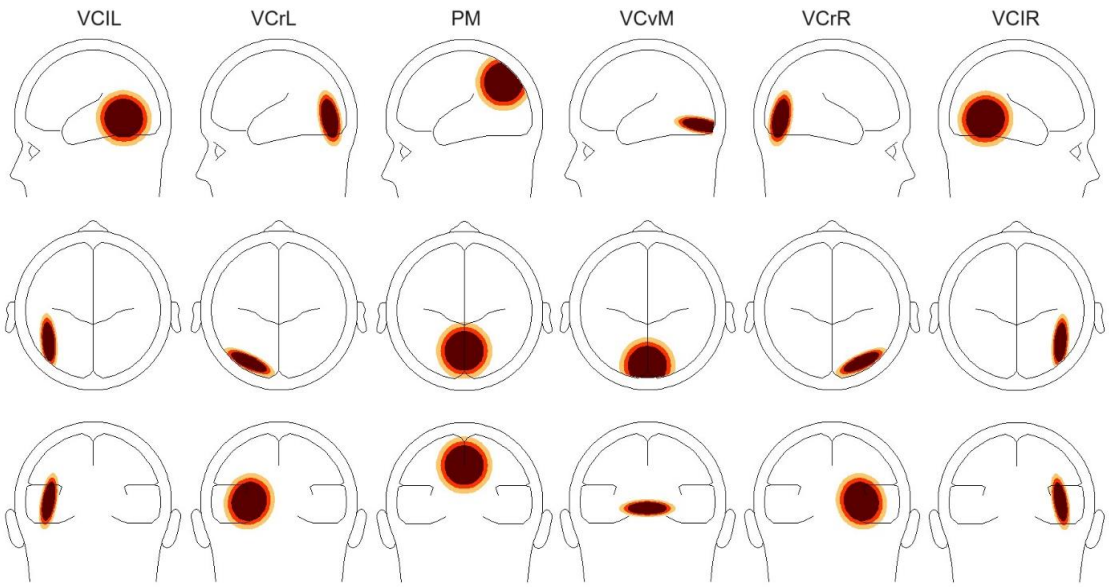

Figure 2: Head model of associated brain regions of interest in visual cortical areas, from left to right VClL, VCrL, PM, VCvM, VCrR, and VClR. The signal magnitude reflects the estimated source activity in the related brain region if one brain region is active.

BESA Statistics 2.1 (BESA, GmbH) was used to assess the probability of significance in amplitude values and frequency ranges between the TSEs of the motion conditions and the static control condition for all infants and children in each group during every testing session, as well as between the TSEs of the full-term and preterm group across motion conditions and the static control condition. The average TSE statistics for participants in each group and each testing session showed significant time-frequency ranges, guiding the identification of patterns in oscillatory activities within each participant's TSE displays. To address the multiple comparisons problem, a data clustering technique in combination with permutation testing was employed (see Bullmore et al., 1999; Ernst, 2004; Maris & Oostenveld, 2007). The rationale underlying this approach is that when a statistical effect is detected across an extended time in several neighboring channels, the likelihood of this effect occurring by chance is reduced. Data clusters demonstrating significant effects between conditions were first defined and assigned initial cluster values, calculated as the sum of all t-values of all data points within the cluster. These initial cluster values were subjected to permutation testing using paired sample t-tests and assigned new cluster values. The significance of the initial clusters was subsequently assessed by examining the distribution of cluster values obtained through permutation for each initial cluster. Permutation was set to 512, with frequency cut-offs consistent with those mentioned above, while the significance level for building clusters in time and/or frequency (cluster alpha) was set to 0.005.

Further, a bootstrapped statistic with a significance level (α=0.05) was computed to explore differences in the TSEs between the motion conditions and the static control condition for each participant in each testing session. The resulting probability maps, which compared conditions separately for each participant in each testing session, enabled the observation of significantly dominant oscillatory activities across the visual area of interest that were not visible in the overall averaged TSEs. To correct for multiple testing, Bonferroni and permutation tests were applied to each set of time samples belonging to one frequency bin. Frequency cut-offs and time-frequency sampling points were maintained as stated earlier.

2.8 Coherence connectivity analysis

Functional connectivity analysis was conducted by applying the coherence method in BESA Connectivity version 2.0. Coherence is a correlation coefficient (squared) that estimates the consistency of relative amplitude and phase between any pair of signals in each specific time-frequency bin (Rosenberg et al., 1989; Srinivasan et al., 2007). Therefore, coherence analysis describes the number of in-phase components of two brain source signals at a specific frequency (Rosenberg et al., 1989; BESA Connectivity information). The same sources montage as in the time-frequency analysis was used in the coherence analysis, focusing on the following sources (Figure 1): VCbL, VClL, VCrL, PM, VCvM, VCrR, VClR, and VCbR.

The computed time-frequency data was utilized for functional connectivity analysis. Coherence connectivity analysis enables the identification of neuronal network activity and connectivity between sources during both visual motion and static control conditions, as well as across ages in both full-term and preterm participants. T-tests were carried out in BESA Statistics 2.1 to assess the probability of significant coherence clusters between conditions, groups, and sessions, followed by a data clustering technique in combination with permutation testing to address the multiple comparisons problem. Permutation was set to 1024, with frequency cut-offs consistent with those in the TSE

analysis, while the significance level for building clusters in time and/or frequency (cluster alpha) was set to 0.05. Paired sample t-tests were carried out to evaluate the probability of significant connectivity between the motion conditions and the static control condition within each group and session.

2.9 Movement ABC

The Movement Assessment Battery for Children (M-ABC) (Henderson et al., 1992) was performed on both full-term and preterm 6-year-old children to assess their motor skills relative to their individual VEP and TSE results. The assessment is designed for use with children aged 4 to 12 years and divided into four age bands, with age bands 4-6 years and 7-8 years utilized in the present study. The structure of the test remains identical across all age bands. M-ABC includes two parts: a performance test involving children performing eight age-appropriate physical test items in a standard way and a checklist completed by a family member regarding the child's day-to-day motor functions, serving as a supplementary tool to evaluate the child's motor abilities in their natural environment. The performance test is categorized into three domains: manual dexterity, ball skills, and static and dynamic balance, with multiple subsets within each domain. The M-ABC manual has different requirements for the different motor tasks and specifies faults of procedure that can result in a child "failing" a task (Henderson et al., 1992). This design provides both qualitative and quantitative aspects of a child's motor performance, as well as emotional and behavioral factors that might influence test performance.

The overall test took approximately 30 minutes for each child. The child's quantitative performance of each physical test item was scored from 0 (best) to 5 (worst). Individual scores were summed to generate a total score, ranging from 0-40. This total score could then be compared to a standardized age group score from Europe for children aged 4 to 12 years. A total score of 13.5 or higher places the child in the category of "clumsiness", indicating having general perceptual-motor problems and placing them among the 5% worst for their age group. A total score between 10 and 13 places the child in a borderline category, requiring monitoring, and situates them among the 15% of the worst for their age group (Henderson et al., 1992).

3 Results

3.1 VEP responses

For each group and each testing session, four posterior electrodes that showed the highest N2 amplitude values for forwards optic flow of the grand average VEPs were selected for further analysis. The four grand average electrodes for full-term infants at 4 months were Pz, POz, PO4, and O2; at 12 months, they were Pz, P2, POz, and O2; and for full-term children at 6 years, the four electrodes were POz, PO4, Oz, and O2. Correspondingly, for preterm infants at 4 months, the four electrodes were P2, POz, PO4, and O2; at 12 months, they were Pz, PO3, POz, and O1; while the electrodes at 6 years of age were Pz, POz, Oz, and O2. The selected electrodes are shown in Figure 3. The grand average VEPs for the three visual motion conditions for each group and each testing session are shown in Figure 4.

Figure 3: The head drawing (nose up) shows the scalp positions of the standard 81 electrodes with electrodes of interest indicated with filled green circles (from top to bottom, left to right): Pz, P2, PO3, POz, PO4, O1, Oz, and O2.

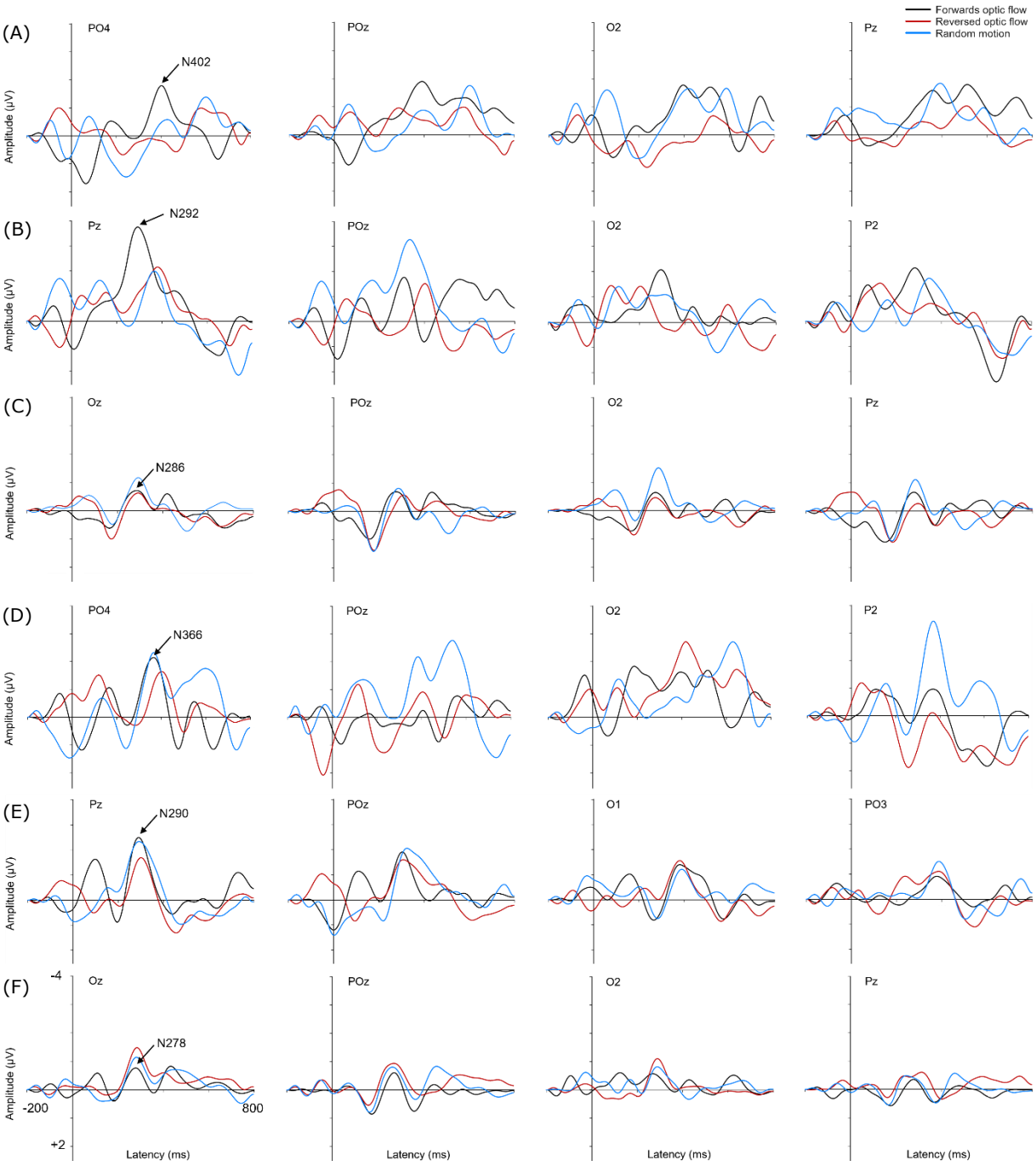

Figure 4: Grand average motion VEPs with epoch from -200 ms to 800 ms in full-term infants and children at 4 months (A), 12 months (B), and 6 years of age (C), and in preterm infants and children at 4 months (D), 12 months (E), and 6 years of age (F). Amplitudes are on the y-axis and latencies on the x-axis. The actual N2 peak latencies for forwards optic flow are indicated at PO4 at 4 months, at Pz at 12 months, and at Oz at 6 years of age in participants.

3.2 Latency and amplitude analyses of VEPs

Repeated-measures ANOVAs were used to separately test for differences in latencies and amplitudes of the VEPs. Within-subjects factor was motion condition (forwards optic flow, reversed optic flow, and random motion) and age (4 months, 12 months, and 6 years of age), while between-subjects factor was participant group (full-term and preterm). Bonferroni correction was used to adjust for multiple comparisons. The one electrode that showed the highest amplitude value in the forwards optic flow among the four electrodes selected in different testing sessions for each participant was used in the analyses. Consequently, while the chosen electrode varied across participants and testing sessions, it was always one of the four posterior electrodes stated above and remained the same for the three motion conditions for each participant.

The mean N2 peak latency for full-term infants at 4 months for the three motion conditions forwards optic flow, reversed optic flow, and random motion was 420 ms (SD=79), 439 ms (SD=88), and 445 ms (SD=76), respectively. Corresponding latencies at 12 months reduced by about 108 ms (SD=37) and were 271 ms (SD=33), 324 ms (SD=30), and 385 ms (SD=45), respectively. Likewise, for full-term children at 6 years, the mean N2 peak latencies for the three motion conditions did not reduce much further and were 271 ms (SD=34), 290 ms (SD=23), and 354 ms (SD=34), respectively. Corresponding latencies for preterm infants at 4 months in the three motion conditions were 345 ms (SD=55), 354 ms (SD=35), and 391 ms (SD=58), respectively. Corresponding latencies at 12 months for preterm infants were quite similar to when they were younger and were 381 ms (SD=57), 376 ms (SD=50), and 398 ms (SD=54), respectively. Finally, preterm children at 6 years showed considerably reduced latencies by about 102 ms (SD=11) and had mean N2 peak latencies of 266 ms (SD=20), 274 ms (SD=21), and 309 ms (SD=38), for forwards optic flow, reversed optic flow, and random motion, respectively (Figure 5).

A significant three-way interaction of motion condition, age and group was found, $F(4, 72)=3.81$, $p<0.01$, $\eta 2=0.18$, indicating significant latency differences between the motion conditions, but only for full-term infants at 12 months and full-term children at 6 years of age (Figure 5). At 12 months of age, full-term infants exhibited a significant increase in latencies from forwards optic flow to reversed optic flow to random visual motion, with an approximate difference of 60 ms between each condition. Similarly, for the same participants at 6 years of age, latencies significantly increased from forwards optic flow to reversed optic flow to random visual motion, with approximately 20 ms between forwards optic flow and reversed optic flow, and 60 ms between reversed optic flow and random visual motion. However, the preterm participants did not differentiate between the three visual motion conditions, neither at 4 months, 12 months, nor at 6 years of age.

Further, the analysis revealed a significant two-way interaction of age and group, $F(2, 36)=11.68$, $p<0.001$, $\eta 2=0.39$, suggesting that there was a significant decrease in latencies for forwards and reversed optic flow for full-term infants from 4 months to 12 months, whereas for preterm participants, the decrease occurred from 12 months to 6 years of age regardless of the visual motion condition (Figure 5). Additionally, preterm participants showed significantly shorter latencies for forwards and reversed optic flow at 4 months and for random visual motion at 6 years of age compared to full-term participants, while full-term infants had significantly shorter latencies for forwards and reversed optic flow than preterm infants at 12 months (Figure 5).

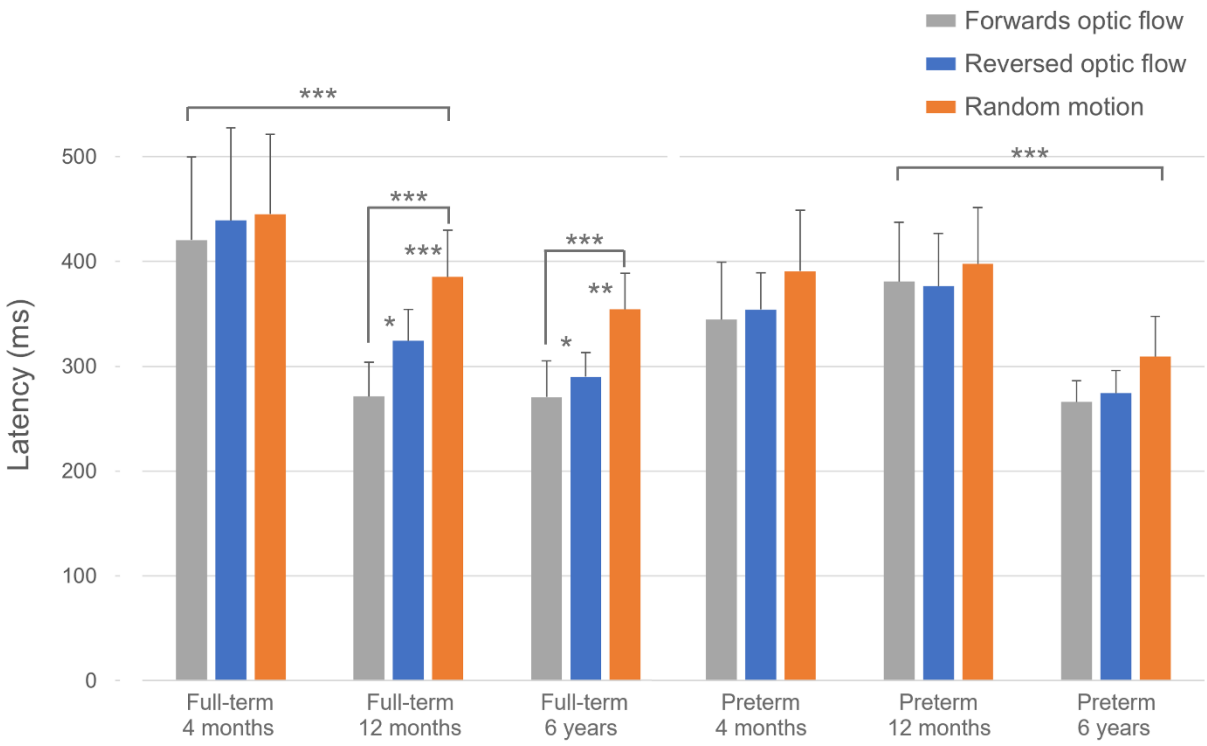

Figure 5: Group means with standard deviations (SDs) of N2 peak latencies for forwards optic flow, reversed optic flow, and random motion in full-term and preterm infants and children at 4 months, 12 months, and 6 years of age. Significant differences in N2 peak latencies for the three motion conditions were observed only in full-term participants at both 12 months and 6 years of age, where latencies significantly increased from forwards optic flow to reversed optic flow to random visual motion. Preterm participants did not differentiate between the three visual motion conditions, neither at the two infant sessions, nor at 6 years of age. Additionally, forwards and reversed optic flow latencies decreased significantly with age for full-term infants from 4 months to 12 months, and for preterm participants, the decrease occurred from 12 months to 6 years of age regardless of the visual motion condition. Preterm participants demonstrated significantly shorter latencies for forwards and reversed optic flow at 4 months and for random visual motion at 6 years of age compared to full-term participants, while at 12 months, full-term infants had significantly shorter latencies for forwards and reversed optic flow compared to preterm infants. *Significant at $p<0.05$, **Significant at $p<0.005$, ***Significant at $p<0.001$.

Mean N2 peak amplitudes for full-term infants at 4 months were 3.86 μV (SD=2.35) for forwards optic flow, 2.95 μV (SD=2.05) for reversed optic flow, and 1.58 μV (SD=1.53) for random motion. The respective amplitudes at 12 months were 2.87 μV (SD=1.30) for forwards optic flow, 2.58 μV (SD=1.96) for reversed optic flow, and 3.12 μV (SD=3.12) for random motion. For full-term children at 6 years of age, the mean amplitudes for the three motion conditions were 0.98 μV (SD=1.39), 0.56 μV (SD=1.16), and 0.85 μV (SD=1.14), respectively. Respective mean N2 peak amplitudes for preterm infants at 4 months in the three motion conditions were 5.17 μV (SD=4.34), 3.94 μV (SD=5.85), and 3.96 μV (SD=4.66). At 12 months, corresponding amplitudes were 3.09 μV (SD=2.56), 3.31 μV (SD=1.74), and 2.18 μV (SD=1.72). For preterm children at 6 years of age, amplitudes in the three motion conditions were 1.42 μV (SD=0.88), 1.20 μV (SD=1.08), and 1.22 μV (SD=1.01), respectively (Figure 6).

Significant main effects were observed for both motion condition $F(2, 36)=3.44$, $p<0.05$, $\eta 2=0.16$ and age $F(2, 36)=10.41$, $p=0.001$, $\eta 2=0.37$ on N2 peak amplitudes, indicating significant higher amplitudes for structured optic flow compared to random visual motion (independent of age and group), and a significant age-related decrease in amplitudes

between 12 months and 6 years across three motion conditions and full-term and preterm participants (Figure 6).

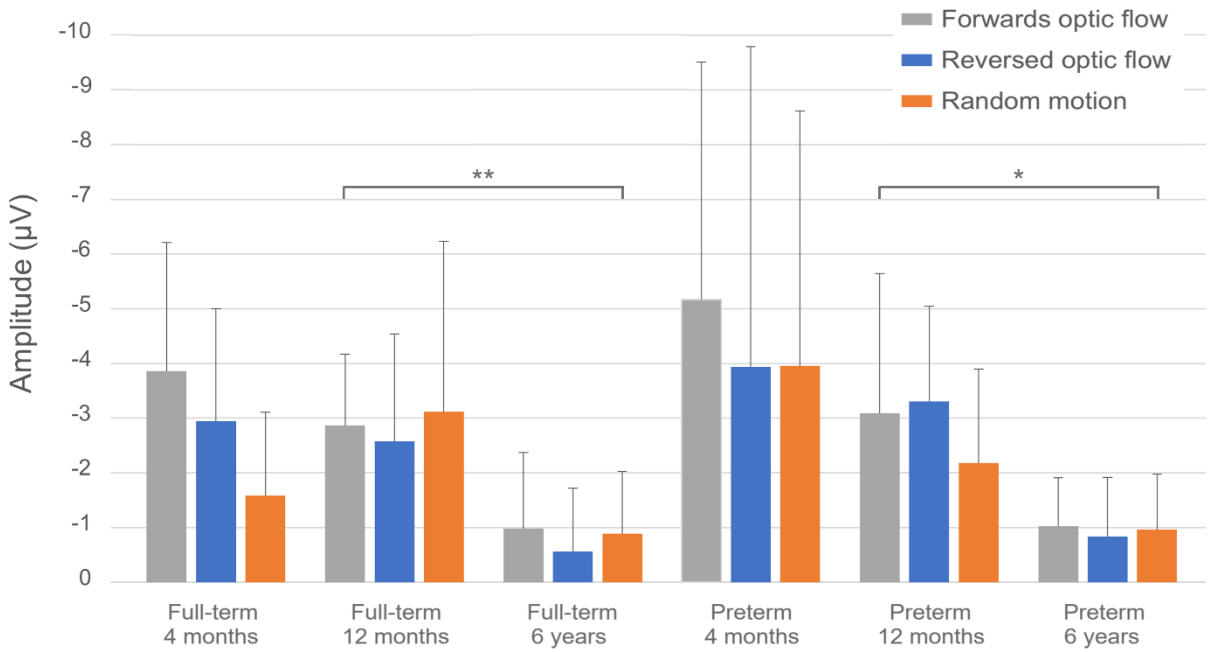

Figure 6: Group means with standard deviation (SDs) of N2 peak amplitudes for three visual motion conditions in full-term and preterm infants and children at 4 months, 12 months, and 6 years of age. Amplitudes were significantly higher for structured optic flow (forwards optic flow and reversed optic flow) compared to random visual motion. Amplitudes decreased significantly with age between 12 months and 6 years. *Significant at $p<0.05$, **Significant at $p<0.005$, ***Significant at $p<0.001$.

3.3 TSE analysis

A time-frequency analysis was carried out for the motion conditions and the static control condition for each participant and the three testing sessions individually. Permutation testing conducted on the TSEs of the three motion conditions for all participants within each group across each testing session revealed no significant differences when comparing them against each other. Therefore, the motion conditions were collapsed into one visual motion condition for subsequent analysis.

Figure 7 illustrates the results of the permutation tests displaying the average for infants and children in each testing session when TSEs for visual motion were compared with the static control condition. The permutation tests showed significant negative clusters (indicating significantly smaller values for motion compared to static) in at least one of the visual areas of interest in both full-term and preterm participants in the three sessions. For each group and in each session, significant negative clusters were identified within at least one of the six regional sources of interest. The results of the permutation tests comparing the visual motion with the static condition revealed significant negative clusters in visual areas, primarily characterized by activity within the theta-band range in both groups at 4 months, and within both theta and alpha-band at 12 months and 6 years of age. Theta-band activity was more prevalent in full-term infants at 12 months (Figure 7B) than in full-term participants at 4 months and 6 years of age (Figure 7A and C), as well as in preterm participants across all sessions (Figure 7D, E and F). Alpha-band activity was most widespread in preterm children at 6 years of age (Figure 7F), followed by full-term and preterm infants at 12 months (Figure 7B and E). The theta-band activity

predominated, occurring over relatively longer periods of time when infants were younger (Figure 7A and D) compared to shorter periods of time as infants in each respective group grew older (Figure 7B and E). As participants aged, alpha-band activity gradually increased and became predominant by the age of 6 years (Figure 7C and F). Additionally, preterm children also exhibited a small amount of beta-band activity (Figure 7F). Similar TSE results were obtained when TSEs of each motion condition were separately compared with those of the static condition.

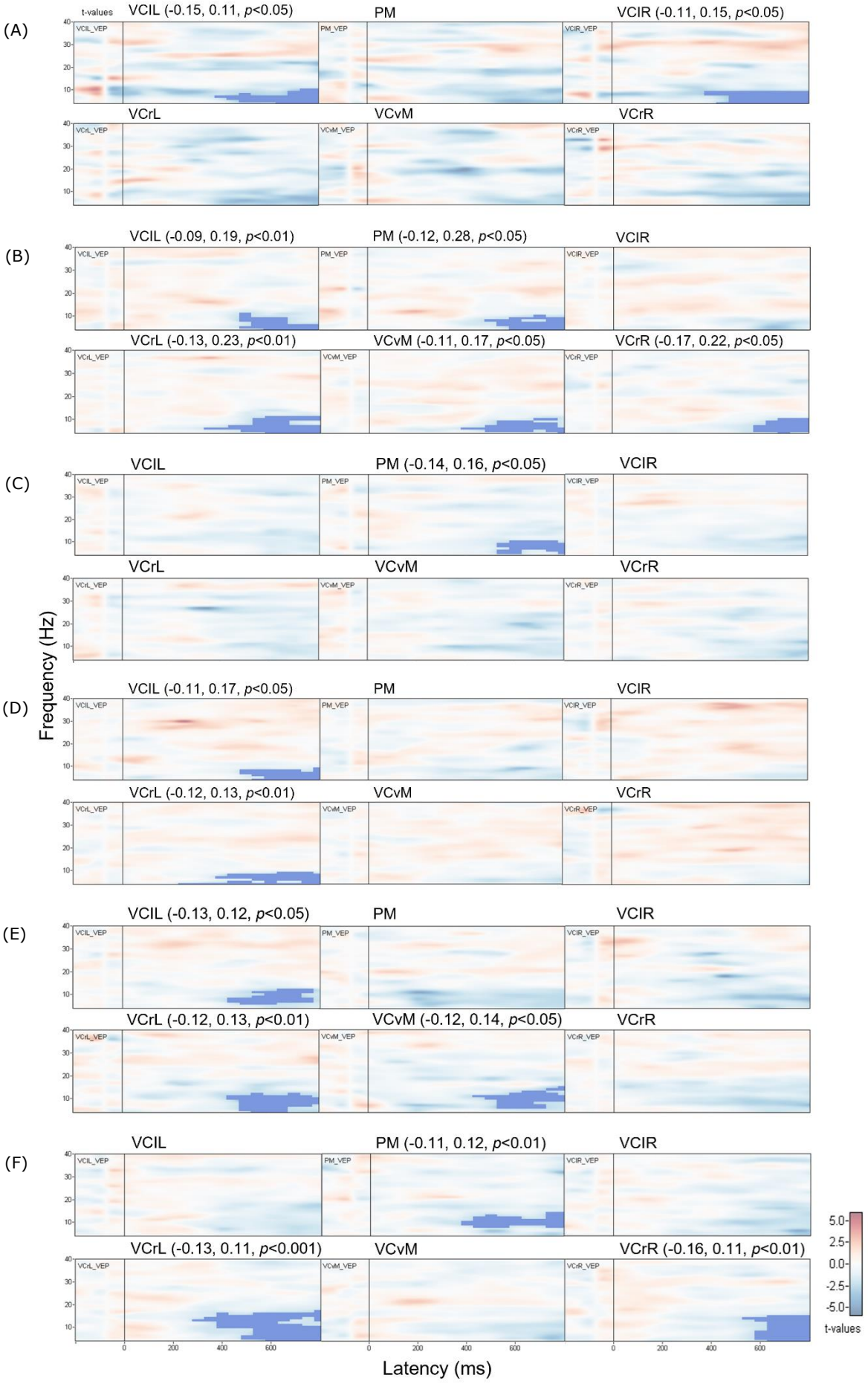
(A)
t-values
VCIL (-0.15, 0.11, p<0.05)
PM
VCIR (-0.11, 0.15, p<0.05)
VCrL
VCvM
VCrR
(B)
VCIL (-0.09, 0.19, p<0.01)
PM (-0.12, 0.28, p<0.05)
VCIR
VCrL (-0.13, 0.23, p<0.01)
VCvM (-0.11, 0.17, p<0.05)
VCrR (-0.17, 0.22, p<0.05)
(C)
VCIL
PM (-0.14, 0.16, p<0.05)
VCIR
VCrL
VCvM
VCrR
(D)
VCIL (-0.11, 0.17, p<0.05)
PM
VCIR
VCrL (-0.12, 0.13, p<0.01)
VCvM
VCrR
(E)
VCIL (-0.13, 0.12, p<0.05)
PM
VCIR
VCrL (-0.12, 0.13, p<0.01)
VCvM (-0.12, 0.14, p<0.05)
VCrR
(F)
VCIL
PM (-0.11, 0.12, p<0.01)
VCIR
VCrL (-0.13, 0.11, p<0.001)
VCvM
VCrR (-0.16, 0.11, p<0.01)
Frequency (Hz)
Latency (ms)
t-values

Figure 7: Average visualization of significant data clusters in the visual sources of interest when the visual motion was compared with the static control condition in full-term infants and children at 4 months (A), 12 months (B), and 6 years of age (C), and in preterm infants and children at 4 months (D), 12 months (E), and 6 years of age (F). Light blue colors represent negative clusters (i.e., smaller t-values for motion compared to static) and positive clusters are marked with light red colors (i.e., larger t-values for motion compared to static). Significant negative clusters ($p<0.05$) in visual areas (VClL, VCrL, PM, VCvM, VCrR, and VClR) are marked with light blue voxel marks. Visual areas were dominated by activity in the theta-band in infancy, but over longer periods of time at 4 months and most prevalent in full-term infants at 12 months. Alpha-band activity gradually increased as participants aged and became predominant by the age of 6 years. A small amount of beta-band activity was observed in preterm children at 6 years of age. In parentheses are the respective cluster means for visual motion, cluster means for static control, and the probability level at which the specific cluster is significant, in that order. Stimulus onset is indicated with a black vertical line at 0 ms with epoch set from -200 ms to 800 ms.

For both full-term and preterm infants at 4 months, TSEs for visual motion displayed lower amplitude values in the theta-band range (Appendix 1A and B) than TSEs of the static control condition (Appendix 1C and D) within the visual areas of interest. The decreased amplitudes in low frequency were observed to be desynchronized with activities induced by motion in both full-term and preterm infants. Thus, from approximately 500 ms to the end of stimulus, suppression of theta-band activity was observed in the visual areas due to the presentation of motion. However, the theta-band desynchronization observed in the TSEs of the visual motion condition contrasted with synchronized theta-band activities in the same time range in the TSEs of the static control condition (Appendix 1). Additionally, these theta-band activities appeared as desynchronized oscillatory activities in the TSEs of both full-term (Figure 8A) and preterm (Figure 8B) infants at 4 months when visual motion was compared with the static control condition. Notably, full-term infants exhibited broader significant desynchronizations in this frequency band.

For both full-term and preterm infants at 12 months, TSEs for visual motion and static control condition yielded similar results to those at 4 months (Appendix 2). However, in response to motion full-term infants displayed some higher synchronized activity in the late alpha and early beta ranges in the TSEs, while preterm infants exhibited desynchronized activity in the alpha-beta band (Appendix 2). Additionally, the observed induced high-frequency synchronized activities in the TSEs for visual motion occurred within the same frequency range as the alpha-beta desynchronized activities in the static control condition. TSEs comparing visual motion to static condition revealed desynchronized oscillatory activities within the theta-alpha band for all infants at 12 months (Figure 9A and B), with synchronized alpha-beta band activity observed only in full-term infants. Furthermore, desynchronized activities in the visual areas peaked later for full-term infants at 12 months compared to preterm infants, occurring from about 650 ms until the end of trials.

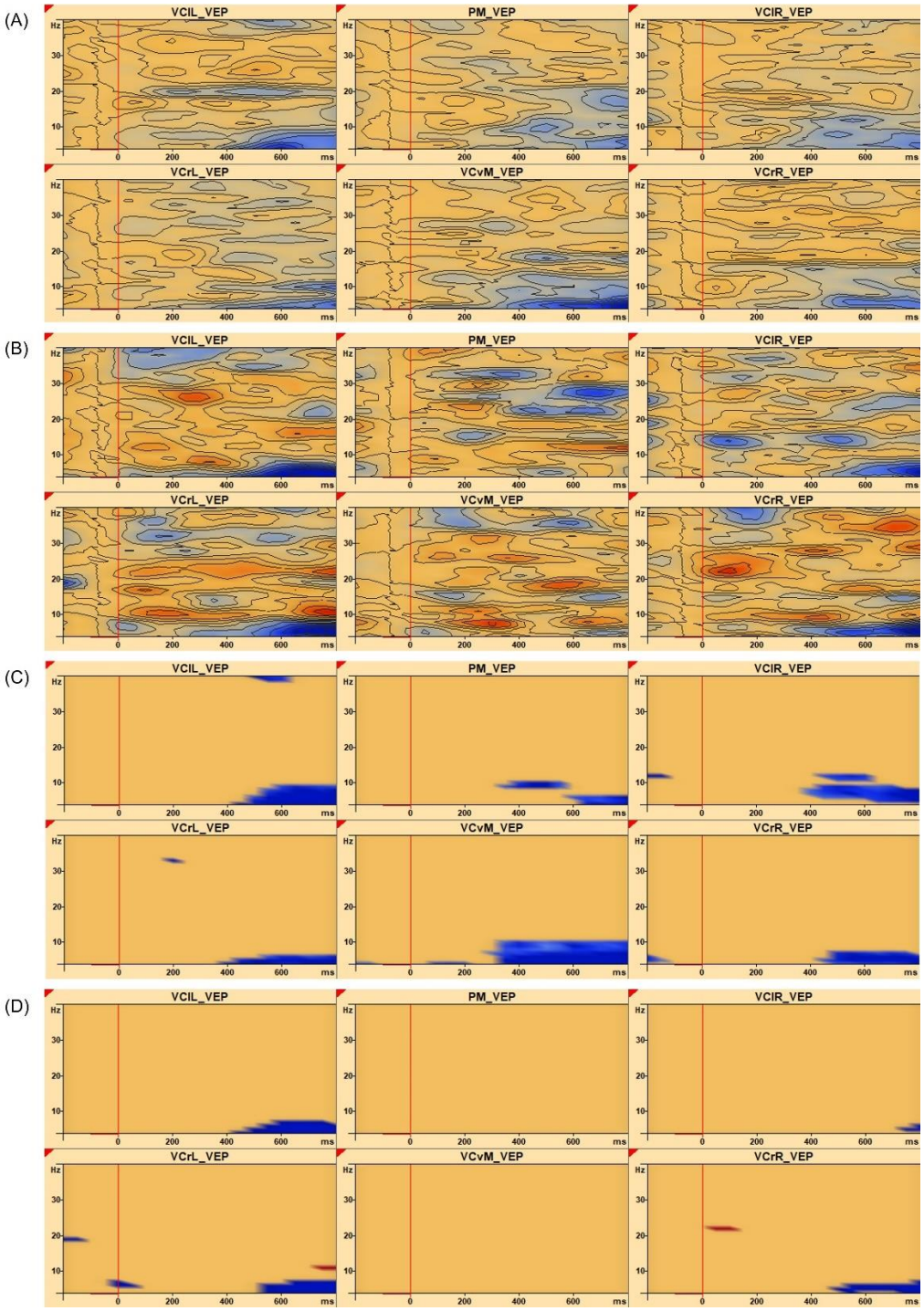

Figure 8: TSE plots (A, B) and TSE probability maps (C, D) across brain regions of interest (VClL, VCrL, PM, VCvM, VCrR, and VClR) at 4 months in full-term infant I (A, C) and preterm infant M (B, D). In the TSE plots, decreased spectral amplitude (induced desynchronized activity) and increased spectral amplitude (induced synchronized activity) are shown in blue and red contours, respectively. Induced theta-band desynchronized activities were predominantly observed in the visual areas of TSEs when comparing visual motion to static control condition, occurring from approximately 500 ms to the end of the trial for both full-term infants and preterm infants. In the TSE probability maps (C, D), significant decrease and increase of TSEs (p<0.05) for visual motion compared to static is shown in blue and red voxel marks. TSE probability maps showed significant induced desynchronization in the theta-band, representing the most pronounced change in activity, while full-term infants exhibited broader significant desynchronizations in this frequency band. Motion onset is indicated with a red vertical line at 0 ms with epoch set from -200 ms to 800 ms and baseline at -100 ms to 0 ms.

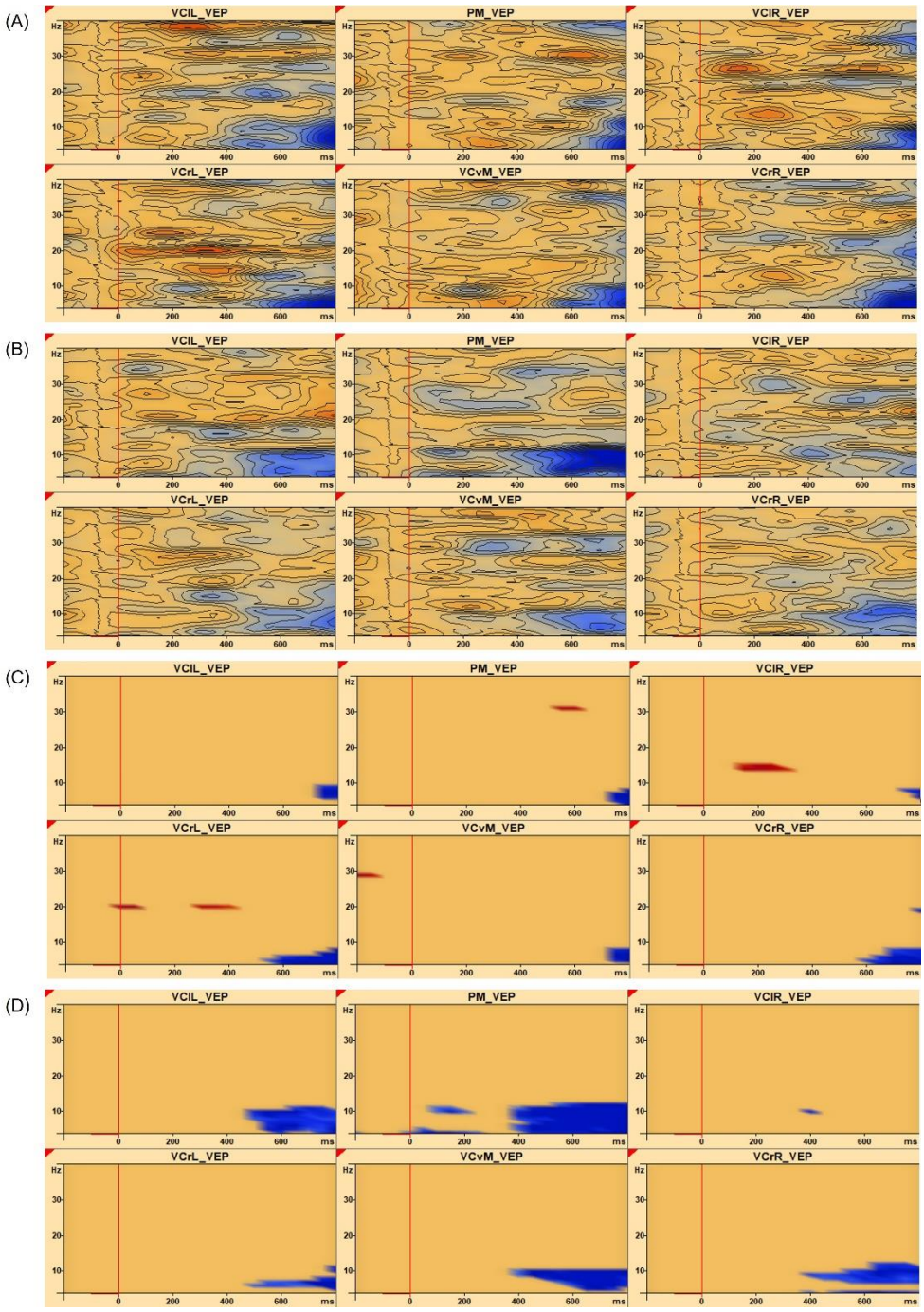

Figure 9: TSE plots (A, B) and TSE probability maps (C, D) across brain regions of interest (VClL, VCrL, PM, VCvM, VCrR, and VClR) at 12 months in full-term infant H (A, C) and preterm infant K (B, D). In the TSE plots, decreased spectral amplitude (induced desynchronized activity) and increased spectral amplitude (induced synchronized activity) are shown in blue and red contours, respectively. Induced theta-alpha band desynchronized activities were predominantly observed in the visual areas of TSEs when comparing visual motion to static control condition, occurring from approximately 650 ms to the end of the trial for full-term infants and from about 500 ms to the end of the stimulus for preterm infants. In the TSE probability maps (C, D), significant decrease and increase of TSEs ($p<0.05$) for visual motion compared to static is shown in blue and red voxel marks. TSE probability maps showed significant induced desynchronization in the theta-band, accompanied by minor desynchronization in the low-frequency alpha-band, representing the most pronounced change in activity. Further, induced amplitude increases in the alpha-beta band were observed only in full-term infants at 12 months (C). Stimulus onset is indicated with a red vertical line at 0 ms with epoch set from -200 ms to 800 ms and baseline at -100 ms to 0 ms.

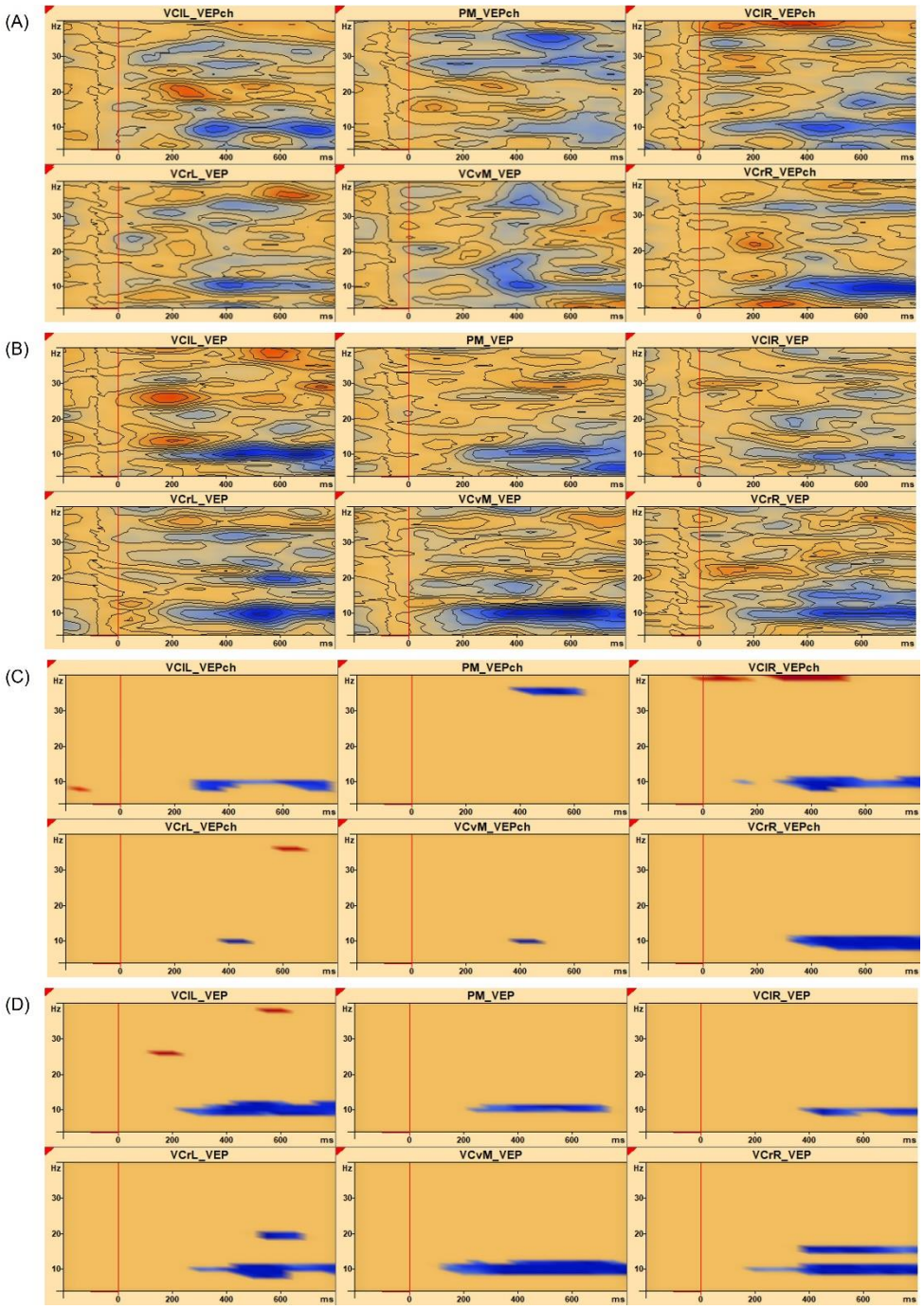

Figure 10: TSE plots (A, B) and TSE probability maps (C, D) across brain regions of interest (VClL, VCrL, PM, VCvM, VCrR, and VClR) at 6 years of age in full-term child H (A, C) and preterm child M (B, D). In the TSE plots, decreased spectral amplitude (induced desynchronized activity) and increased spectral amplitude (induced synchronized activity) are shown in blue and red contours, respectively. Induced alpha-beta band desynchronized activities were predominantly observed in the visual areas of TSEs when comparing visual motion to static control condition, occurring from approximately 300ms to the end of the trial for both full-term and preterm children. Induced synchronizations within the beta and early gamma band ranges in different epochs were shown, particularly for the full-term children. Unlike infants, fewer or no theta-band activities were observed for both full-term and preterm children at 6 years of age. In the TSE probability maps (C, D), significant decrease and increase of TSEs ($p<0.05$) in the visual motion compared to static is shown in blue and red voxel marks. TSE probability maps showed significant induced desynchronization in the alpha-beta band, accompanied by minor synchronizations in the beta and early gamma band in both groups. Stimulus onset is indicated with a red vertical line at 0ms with epoch set from -200ms to 800ms and baseline at -100ms to 0ms.

At 6 years of age, both full-term and preterm children exhibited desynchronized oscillatory activities in the TSEs for visual motion and synchronized oscillatory activities for static control condition within the late alpha and early beta ranges of the visual areas of interest (Appendix 3). These activities were more pronounced in preterm children than in full-term children (Appendix 3). TSEs comparing visual motion to the static control condition not only revealed desynchronized oscillatory activities within the late alpha and early beta bands from 300ms to the end of stimulus but also indicated higher synchronizations within the beta and early gamma band ranges in different epochs (Figure 10A and B), particularly for full-term children. Unlike infants at 4 months and 12 months, fewer or no theta-band activities were observed for both full-term and preterm children at 6 years of age.

Further statistical analysis of each participant when comparing the TSEs of the visual motion with TSEs of the static control condition revealed significant activities similar to those shown in the TSEs of the comparison between these two conditions (Figure 8C and D, 9C and D, 10C and D). In particular, prominent high-amplitude oscillatory activities were observed in two or more visual areas of interest in the full-term participants at 12 months and 6 years of age (Figure 9C and Figure 10C), while they were observed only in one of the visual areas of interest in preterm children at 6 years of age (Figure 10D). These high amplitudes within the alpha, beta, and early gamma frequency bands occurred in different epochs in the probability maps. In contrast to older full-term infants and children, where high-frequency synchronized activities were prominent, some preterm participants at 12 months (3 out of 10) and 6 years of age (5 out of 10) showed significant high-frequency synchronized activities, particularly in the beta-band. Additionally, no significant differences in induced activities were found when TSEs were compared between the motion conditions in each participant. In the TSEs of each participant and in the TSEs of each age group, no significant induced activities in any other frequency bands were observed when frequency cut-off was analyzed below 4 Hz and above 40 Hz.

3.4 Individual analyses of VEPs, TSEs, and M-ABC

Individual analyses were conducted on the VEP latency values for full-term and preterm infants at 12 months, as well as when they were 6 years of age, considering that significant differences between the three visual motion conditions were solely observed in full-term participants at 12 months and 6 years of age, with no such differences noted in preterm participants at any of the ages tested. The individual analysis aimed to identify a criterion capable of distinguishing preterm participants exhibiting extreme delays in their VEP responses from the other full-term and preterm participants at these ages. TSEs comparing visual motion to static control condition and locomotor ability evaluation of each participant at 12 months and 6 years of age, were also scrutinized to investigate potential links between induced frequency changes of neural oscillations, perceptuo-motor functioning, and the N2 component.

Field (2013) defined an outlier of latency as the value that was smaller or larger than the mean±SD*2.5 of a reference value. The VEP latency values of the three motion conditions were separately calculated for full-term infants and children at 12 months and 6 years of age, serving as the references for comparison within each respective age group. The criterion identified four preterm infants M, O, Q, and T with outlier latency values for both forwards optic flow and reversed optic flow at 12 months, exhibiting longer latencies than the mean + SD*2.5 of the average VEP latency (Table 1). Three

additional preterm infants L, N, and P also showed outlier latency values observed exclusively for forwards optic flow (Table 1). Among them, two were identified as bottom shufflers, while the third infant is the girl who suffered a brain hemorrhage (grade 3) during her first week of life. None of these preterm infants with outlier latency values showed delayed motor responses at the time of the second testing at 12 months. TSE analysis in preterm infants K, R, and S at 12 months, without outlier latency values for both forwards optic flow and reversed optic flow, demonstrated desynchronized oscillatory activities within the theta-alpha band more akin to full-term infants at 12 months. Conversely, theta-band desynchronization ranging from approximately 300 ms to 800 ms was prominent in other preterm infants (infants M, N, O, and T), who exhibited outlier latency values when TSEs of visual motion compared to static control condition. Notably, at 12 months, full-term infants exhibited an average latency approximately 110 ms earlier for forwards optic flow and approximately 60 ms earlier for reversed optic flow compared to preterm infants, while showing similar latencies for random visual motion. Full-term infants showed latency differences between structured optic flow and random motion, whereas preterm infants exhibited more similar latencies across the three conditions (Table 1).

At 6 years of age, the results showed neither full-term nor preterm children had latency values higher than the criterion for the three motion conditions (Table 2). Furthermore, upon closer examination of the VEP latencies within the preterm group, individual analyses revealed that preterm children exhibited a tendency to differentiate between the three motion conditions. All preterm children (except possibly child N) displayed shorter latencies for structured optic flow and longer latency for random visual motion. Among these, five preterm children (children K, L, M, R, and T) increased their latencies from forwards optic flow to reversed optic flow to random visual motion. Importantly, all of the preterm children exhibited the shortest latency for forwards optic flow. TSEs comparing visual motion to static in preterm children who showed a tendency to differentiate between the three motion conditions revealed desynchronized oscillatory activities within the late alpha and early beta bands, but with minimal synchronizations within high-frequency ranges compared to full-term children. Notably, preterm child N, who suffered a brain hemorrhage in the first week of life, still exhibited minimal theta-band desynchronization in two visual areas of interest.

Additionally, M-ABC was conducted on children at 6 years of age (with one full-term child, G, missing the test) to assess potential differences in motor function between full-term and preterm children at this age. The study also aimed to determine whether the same preterm children who scored high on the M-ABC exhibited longer latency values at 12 months or at 6 years of age. An independent-sample t-test revealed no significant differences in M-ABC scores between full-term and preterm children. The M-ABC showed that three children in each group scored above 10 points, placing them within the bottom 15% of their age group, suggesting the need for monitoring these children. Among these children, one full-term and two preterm children had a score above 13.5, suggesting they belong within 5% of the weakest in their age group. Preterm child R, who showed acceptable latencies at 12 months within the normal range, attained the poorest M-ABC score of 22 points, while preterm child Q was the sole participant who both showed delayed responses to optic flow at 12 months and had poor scores on the M-ABC test at 6 years of age (see Table 1 and 2).

Table 1: VEP latencies (ms) of the visual motion conditions for full-term infants (A-J) and preterm infants (K-T) at 12 months of age. Preterm infants M, O, Q and T showed latency values for both forwards and reversed optic flow that were larger than mean+SD*2.5 of the average latency values of the corresponding optic flow conditions in the full-term infants. GA=gestational age in weeks^{+days}.

Full-term infants	GA	Forwards optic flow	Reversed optic flow	Random visual motion	Preterm infants	GA	Forwards optic flow	Reversed optic flow	Random visual motion
A	40	300	314	456	**K**	32^{+5}	306	344	372
B	40	320	310	392	**L**	28^{+3}	**384**	372	414
C	39^{+4}	264	280	398	**M**	30	**486**	**424**	466
D	41^{+6}	280	320	438	**N**	26^{+1}	**424**	386	360
E	39	238	364	394	**O**	33	**402**	**404**	378
F	40	250	342	324	**P**	32^{+3}	**398**	332	386
G	41^{+3}	210	376	410	**Q**	31^{+3}	**376**	**414**	476
H	41^{+4}	272	312	372	**R**	32^{+4}	320	354	348
I	41^{+6}	302	292	324	**S**	32^{+5}	308	282	318
J	41^{+3}	276	332	344	**T**	32^{+6}	**404**	**452**	458
Mean		271	324	385					
SD		33	30	45					
Mean+ (SD*2.5)		354	399	498					

Table 2: VEP latencies (ms) of the visual motion conditions and M-ABC scores for full-term children (A-J) and preterm children (K-T) at 6 years of age. None of the preterm children showed latency values exceeding the mean+SD*2.5 of the average latency values of the corresponding optic flow conditions in the full-term children. All preterm children (except possibly child N) exhibited a tendency to differentiate between structured optic flow and unstructured random visual motion. Five of these preterm children increased their latencies from forwards optic flow to reversed optic flow to random visual motion. All participants exhibited the shortest latency for forwards optic flow. The average M-ABC scores did not significantly differ between full-term and preterm children. In each group, three children scored above 10 points, positioning them within the bottom 15% of their age group. Among these children, one full-term and two preterm children scored above 13.5, indicating placement within the bottom 5% of their age group. Preterm child Q and R achieved the highest M-ABC score of 21 and 22 points, respectively. GA=gestational age in weeks^{+days}.

Full-term children	GA	Forwards optic flow	Reversed optic flow	Random visual motion	M-ABC	Preterm children	GA	Forwards optic flow	Reversed optic flow	Random visual motion	M-ABC
A	40	264	296	374	**14**	**K**	32^{+5}	288	292	322	5
B	40	226	300	402	0	**L**	28^{+3}	254	274	276	3.5
C	39^{+4}	220	250	386	**10**	**M**	30	260	280	298	5.5
D	41^{+6}	306	314	312	9	**N**	26^{+1}	278	302	280	7.5
E	39	250	272	340	0	**O**	33	262	244	266	4
F	40	242	280	348	6	**P**	32^{+3}	272	260	368	4
G	41^{+3}	294	272	378		**Q**	31^{+3}	284	284	292	**21**
H	41^{+4}	312	328	380	5	**R**	32^{+4}	276	300	302	**22**
I	41^{+6}	292	284	320	**12**	**S**	32^{+5}	268	266	306	**13**
J	41^{+3}	300	304	304	9	**T**	32^{+6}	218	242	382	2
Mean		271	290	354							
SD		34	23	34							
Mean+ (SD*2.5)		356	348	439							

3.5 Coherence connectivity analysis

As in the TSE analysis, no significant connectivity differences between the three motion conditions were found, thus, the three motion conditions were combined into a unified visual motion condition for subsequent analysis. To examine significant connectivity differences between visual motion and static control condition in full-term and preterm participants across three testing sessions, paired sample t-tests were conducted on coherence connectivity patterns. The results were visualized using the head model with sources of interest, as depicted in Figure 11. At 4 months, no significant clusters were found between motion versus static for either full-term or preterm infants. At 12 months, a significant positive cluster in beta-band was observed between visual motion and static in full-term infants, whereas no significant cluster was detected between the two conditions in preterm infants. Later, at 6 years of age, both groups exhibited significant cluster differences between motion versus static. Full-term children displayed five significant connectivity differences in the alpha-beta band localized in the occipital and parietal regions, including four interactions with PM and VCvM sources in the lower dorsal stream. In contrast, preterm children demonstrated one significant connectivity difference in beta-band in the visual areas of interest. These findings suggest that, compared to their preterm counterparts, full-term participants exhibited earlier and more robust functional connectivity, particularly involving higher visual areas, when processing motion stimuli compared to static stimuli at 6 years of age.

Furthermore, no significant connectivity differences were observed between full-term and preterm participants in both visual motion and static control condition across three testing sessions.

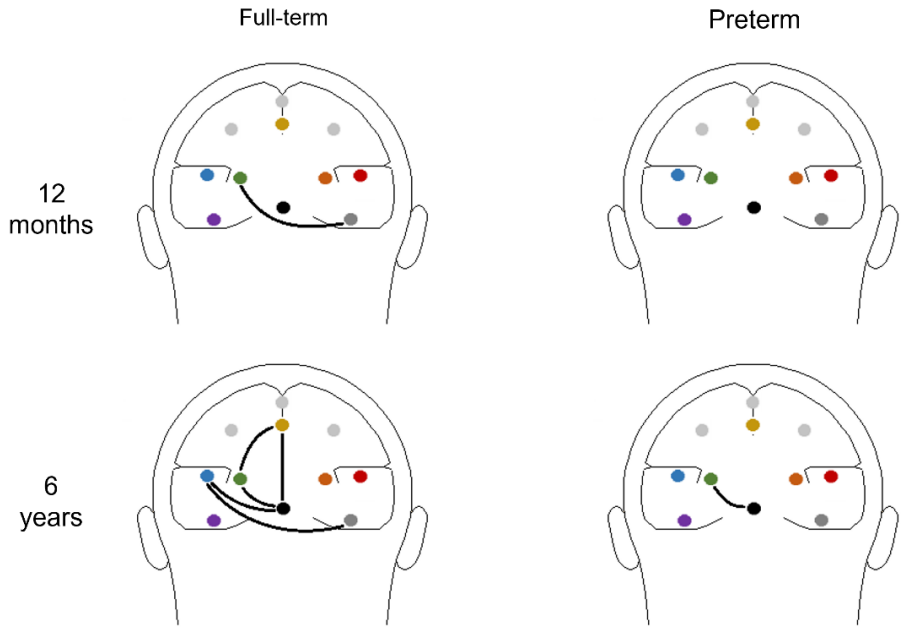

Figure 11: Head model with significant coherence connectivity differences (p<0.05) when visual motion compared to static within the groups of full-term (left) and preterm (right) participants at 12 months (top) and 6 years of age (bottom). At 12 months, a significant positive cluster in beta-band was observed in full-term infants, whereas no significant cluster was detected in preterm infants. At 6 years of age, full-term children displayed five significant connectivity differences in the alpha-beta band localized in the occipital and parietal regions, including four interactions with PM and VCvM sources in the lower dorsal stream. In contrast, preterm children demonstrated just one significant connectivity difference in beta-band in the visual areas of interest.

4 Discussion

The present longitudinal study investigated the development of visual motion perception from early infancy up to six years of age, and the differences in processing visual motion information between full-term and preterm individuals. Using high-density EEG, brain electrical activity in response to structured radial optic flow (forwards and reversed) and random visual motion was observed at 4 months, 12 months, and 6 years of age. Motion-specific N2 component of the VEP waveforms were compared for latencies and amplitudes. Induced oscillation activities across various frequency bands over time and the functional connectivity of networks were further analyzed.

VEP analysis revealed a significant decrease in latencies for full-term infants from 4 months to 12 months, especially for structured optic flow. Additionally, a significant improvement in latencies from forwards optic flow to reversed optic flow to random visual motion were observed only in full-term participants at 12 months and at 6 years of age. However, at 4 months, there were no noticeable differences in latencies between the motion conditions for full-term infants. The finding of shorter latencies for structured optic flow and longer latency for random visual motion aligns with previous studies employing similar experimental paradigm in full-term infants aged 4 to 12 months (Agyei et al., 2015; 2016a; Borge Blystad & Van der Meer, 2022; Van der Meer et al., 2008). Ongoing neural maturation could partly explain the more efficient processing of visual motion in normally developing full-term infants from 12 months. Studies have reported a rapid increase in white matter volume primarily due to the myelination of axons and increasing fiber compaction during the early postnatal period, and these changes continue throughout childhood until late adolescence (Casey et al., 2000; Loenneker et al., 2011; Paus et al., 2001). The formation of myelin sheaths around axons by oligodendrocytes leads to the improved conduction velocity of electrical impulses and increased efficiency of neural communication within the brain (Fields, 2008). Thus, myelination facilitates the efficient propagation of visual information, leading to shorter latencies of the N2 component for motion perception in full-term infants at 12 months compared to when they were 4 months old, particularly for structured radial optic flow. In addition, the number, size, and complexity of dendrites increase and reach a peak level between the ages of 8 months and 2 years (Bourgeois & Rakic, 1993; Cichocka & Bereś, 2018; Klaver et al., 2011). Meanwhile, the density of synapses in the primary visual cortex increases and reaches the mean maximum density by the third postnatal month, with a subsequent decrease occurring between 2.7 and 5 years (Bourgeois & Rakic, 1993; Klaver et al., 2011). Further, it has also been revealed that the rate of metabolic activity in cerebral cortex and white matter increases remarkably from 40 weeks of gestation to 1 year of age, continuing to increase until adolescence/adulthood before decreasing (Cichocka & Bereś, 2018; Kato et al., 1997). Hence, these changes in dendrites, synaptic connections, and metabolic activity may underlie the functional specializations of neurons, particularly supporting the development of the dorsal visual stream. These improvements gradually reach their peak around half a year after birth, which may explain why the ability to differentiate between different forms of visual motion in the present study was only observed in full-term individuals from 12 months, not at 4 months.

Full-term infants exhibited shorter N2 latencies for forwards and reversed optic flow at 12 months, and for random visual motion at 6 years of age, compared to when they were 4 months old. Infants' faster responses to structured visual motion may be attributed to their frequent exposure to structured information from daily experiences (Bruggeman & Warren, 2010; Johnson, 2010; Lamontagne et al., 2007). After birth, infants begin to passively experience similar structured optic flow patterns as their parents when they are carried in a forward-facing carrier, held in their mothers' arms, or pushed in a stroller (Raudies et al., 2012). They begin to explore their environment through independent movement when they start to crawl or walk. It has been revealed that prior to the onset of locomotion, there is minimal development in sensitivity to optic flow between 3 to 6 months (Gilmore et al., 2004). Therefore, having only passive experiences could account for the longer latencies and inability to differentiate between the different forms of visual motion at 4 months. Additionally, this provides a basis for the development of motion perception associated with the dorsal visual stream, which may depend on locomotor experience. Poor performance on discriminating optic flow patterns has been demonstrated in 4-month-olds infants before crawling (Gilmore & Rettke, 2003). EEG studies with infants receiving extra motor stimulation, such as swimming, have shown greater improvement in visual motion perception during the first year than a control group of full-term infants who did not attend swimming classes (Borge Blystad & Van der Meer, 2022). Behavioral studies have demonstrated that the ability to perceive optic flow is present in infants before they begin to sit independently, and it showed considerable improvement when infants learn to sit and crawl (Bertenthal et al., 1997; Rinaldi et al., 2009). Evidence from computational modeling has shown that neural networks learn to coordinate vision and reaching during bouts of exploration of the environment (Johnson, 2010). These findings support a close link between the perception of optic flow and self-generated locomotion, indicating that infants sensitive to perceiving optic flow and scaling posture become more finely tuned with accumulated locomotor experience (Bertenthal et al., 1997). Hence, self-generated locomotion experience may play a more significant role in the normal development of visual perception compared to passive experience. Neurophysiological research has found that sensory processing in the visual cortex is more influenced by movement state compared to when at rest, potentially optimizing visual perception during active exploration of the environment (Niell & Stryker, 2010). Moreover, functional perception of structured radial flow develops as independent locomotion is acquired (Agyei et al., 2015; 2016a; Borge Blystad & Van der Meer, 2022; Van der Meer et al., 2008). In the present study, all full-term infants had approximately 3 months of crawling experience, and some of them could independently pull to stand, or walk by the testing at 12 months of age. It is reasonable to assume that, apart from maturation, the accumulated self-locomotion experience may have led to faster activation and greater specialization of neural networks responsible for structured motion perception compared to younger infants who have only experienced passive motion. However, for random visual motion, due to limited relevant life experiences, neural networks lack corresponding pruning and shaping at the first year of life, resulting in the observed small decrease in N2 latencies in response to random visual motion at 12 months. With increasing exposure to random visual motion, full-term children exhibited a notable improvement in latency during early childhood.

VEP results revealed that preterm participants did not exhibit a significant decrease in latencies from 4 months to 12 months, nor did they differentiate between the three visual motion conditions at any of the testing ages (4 months, 12 months, and 6 years). Even though preterm infants had similar number of months of locomotor experience as

their full-term peers at 12 months and showed no significant difference in M-ABC test at 6 years of age, they were not as capable as the full-term infants in differentiating between the different forms of visual motion. This is corresponding with previous studies in preterm infants (Agyei et al., 2015; 2016a; Borge Blystad & Van der Meer, 2022), and children (Taylor et al., 2009; Guzzetta et al., 2009). Apart from the inability to differentiate between optic flow (Agyei et al., 2015; 2016a; Borge Blystad & Van der Meer, 2022), a delayed maturation of directional motion processing has also been shown in preterm infants at a corrected age of 2-4 months (Birtles et al., 2007). Even at school age, premature children continued to exhibit decreased sensitivity in perceiving optic flow compared to controls (Guzzetta et al., 2009; Taylor et al., 2009). Most neuroimaging studies support the notion that abnormality in cerebral white matter at various ages are associated with preterm birth (Atkinson et al., 2008; Counsell & Boardman, 2005; Sripada et al., 2015). Further, neuropsychobehavioural follow-up studies have found that cerebral white matter abnormality characterized by diffuse and excessive high signal intensity (DEHSI), should be regarded as indicators of white matter injury rather than delayed maturation (Domizio et al., 2005). Several lines of evidence suggest that inadequate receiving of docosahexaenoic acid (DHA) may lead to impaired motion perception, as DHA appears to be particularly important for the visual functions subsumed by the magnocellular and dorsal stream (Molloy et al., 2012; O'Connor et al., 2001). During the last trimester of pregnancy, a substantial amount of DHA is transferred from mother to fetus; thus, infants born earlier than 32 weeks gestational age may experience insufficient intrauterine supply of DHA at a stage when brain growth is at its peak (Molloy et al., 2012). Therefore, it is conceivable that white matter impairment or DHA deficiency resulting from premature birth leads to no improvement in latencies and an inability in differentiation between the different forms of visual motion for preterm infants at 12 months. Whether these functions can be restored with age or if it represents a typical delay, the present follow-up study monitoring the developmental progress of preterm infants has provided some evidence. At 6 years old, preterm children exhibited a significant decrease in latency, reaching the level of full-term children, compared to their latency at 12 months old. Additionally, the majority of preterm children displayed a tendency to differentiate between structured optic flow and random visual motion. Other studies on preterm children have indicated that while they did not perform worse than from full-term children in form perception, their performance in motion perception remains inferior to that of full-term children (Guzzetta et al., 2009; Taylor et al., 2009). These findings indicate that functional deficits stemming from preterm birth, associated with impairments of the dorsal pathway and white matter, emphasize the vulnerability of the dorsal stream in preterm individuals. These functional deficits may improve somewhat with age, highlighting the prolonged maturation and plasticity process of the dorsal stream.

Interestingly, preterm participants showed significantly shorter latencies for structured optic flow at 4 months and for random visual motion at 6 years of age compared to full-term participants. Preterm participants in the present study were corrected for prematurity, which could have contributed to the faster response of preterm infants at 4 months, as they had up to 3 months longer exposure and experience to real-world visual flow than the full-term infants. At 6 years of age, preterm children shortened their latencies to the level of the full-term children, potentially reflecting accelerated maturation or compensatory mechanisms of visual system from late infancy to childhood. Additionally, the environment provided to preterm children may have contributed to their improvement. Individual analysis of the preterm participants further pointed to seven

infants who showed outlier latency values for structured optic flow, while none of these preterm infants exhibited delayed motor responses at 12 months. At 6 years of age, none of the preterm children had outlier latency values, and almost all preterm children exhibited a tendency to differentiate between structured optic flow and unstructured random visual motion, although three of them had poor M-ABC scores. These results suggest that the poor performance in latency and differentiating different forms of visual motion may be normal developmental delays that gradually recover with age.

Comparison of the amplitudes of N2 component revealed lower activation values for structured optic flow compared to random visual motion and lower activation values between 12 months and 6 years across three different forms of visual motion for both full-term and preterm participants. The amplitude of brain electrical waveforms reflects the magnitude of response from excited neurons, with a larger amplitude indicating a stronger or more synchronized neural response to the stimulus (Regan, 1989). Compared to random visual motion, the lower amplitude for structured optic flow may reflect fewer synchronously activated neurons responding to the visual motion. This suggests that neurons have become more adapted to optic flow due to increased life experience compared to random motion. The lower amplitudes observed at 6 years of age compared to 12 months also reflect the maturation of the visual cortex. This difference may be influenced by the relatively thicker skulls after the first year of life, which allow for greater diffusion and impedance when measuring cortical electrical activity (Grieve et al., 2003). However, the amplitudes recorded for all participants from infancy to early childhood were generally higher when compared to adults' amplitudes (Van der Meer et al., 2008; Vilhelmsen et al., 2019). One contributing factor to these large activation values could be less specialized and adapted neural networks in visual motion perception in infants and children.

Investigating the differences in induced activities revealed that when comparing the TSEs of visual motion (forwards and reversed optic flow, and random visual motion) to a static control condition, both full-term and preterm infants at 4 months exhibited low-amplitude values in the theta-band range, observed as desynchronized activity over the visual areas of interest. Moreover, TSEs comparing motion to static unveiled desynchronized oscillatory activities within the theta-alpha band for all infants at 12 months, and within the late alpha and early beta bands for both full-term and preterm children at 6 years of age. These studies corroborate previous TSE findings, revealing induced desynchronized activities in the theta-band range for younger infants, transitioning to the theta-alpha band range for older infants, and further extending into the alpha and beta ranges for children for motion perception (Agyei et al., 2015; 2016a; Borge Blystad & Van der Meer, 2022; Rasulo et al., 2021). Studies have reported that changes in neural oscillations in infants are dominated by large amplitude waveforms with low frequency, serving as a general sign of immaturity (Orekhova et al., 2006; Pfurtscheller et al., 1994; Thierry, 2005). At low frequencies, slowly oscillating patterns typically occur, involving very large populations of cells discharging in unison, in contrast to faster oscillating cell assemblies, with amplitude of oscillation being proportional to the number of synchronously firing neurons (Elul, 1972; Pfurtscheller & Da Silva, 1999; Pfurtscheller et al., 1994; Singer, 1993). At these low frequencies, self-generated rhythmic discharges are scarcely influenced by sensory stimuli (Singer, 1993). Thus, the prevalent desynchronized theta-band activity in infants may suggest recruitment of larger neurons and less specialized cortical networks during the processing of motion information. Additionally, given that infancy is a period of rapid synapse formation in the brain (Casey et al., 2000), the observation of theta-band activities in infants could reflect the plasticity of cortical

synapses involved in processing motion information. Given that theta-band oscillatory activities were present in all infants at both 4 and 12 months in response to visual motion, oscillatory activities within the theta-band frequency may represent a common characteristic of immature neuronal networks responsible for processing motion information during the first year of life. Desynchronized theta-band activities are more prevalent in infants compared to children in both full-term and preterm participants, with an extension in frequencies from theta-band to beta-band of desynchronization observed. This progression from lower to higher frequencies in response to visual motion can be linked to an increase in visual experience in participants from infancy to early childhood (Orekhova et al., 2006; Stroganova et al., 1999). With increasing age and more experience, there is a transition from larger and less specialized oscillatory cell assemblies in younger infants to fewer and more specialized neuronal networks.

Notably, desynchronized activity was observed within both theta and alpha bands in both full-term and preterm infants at 12 months, which does not entirely corroborate earlier findings that only theta-band desynchronization was exhibited. Better task performance, or more attention needed, lead to an enhancement in alpha desynchronization (Pfurtscheller & Lopez da Silva, 1999). The differences in task performance, the level of attention to visual motion, and the degree of specialization in neural networks between participants in the present study and previous studies may offer possible explanations for the discrepancy in the results.

At 4 months, full-term infants exhibited broader and longer low-frequency desynchronizations across more visual areas of interest compared to preterm infants. Conversely, at 12 months, low-frequency desynchronizations covered a longer period in preterm infants compared to full-term infants. This finding further explains the differences in N2 latency. Compared to preterm infants, who exhibited relatively faster latency to visual motion, full-term infants at 4 months have less specialized and larger cortical neuronal networks, resulting in slower perceptual responses (longer N2 latency). In contrast, at 12 months, the neural networks in full-term infants have undergone more development, requiring fewer neurons and becoming more specialized for processing visual motion. As a result, compared to preterm infants, full-term infants exhibit shorter N2 latencies and begin to demonstrate the ability to differentiate motion conditions. Interestingly, at 12 months, full-term infants exhibited significantly lower amplitude values in the theta-alpha band ranges, observed as desynchronization when comparing motion to static. This observation may suggest the recruitment of larger neuron assemblies to form a specialized cortical network, enabling the ability to differentiate between motion conditions (Agyei et al., 2016a).

High-amplitude values in the alpha-beta frequency band were found in full-term infants at 12 months, while higher synchronizations were observed within the beta and early gamma band ranges in 6-year-old children, particularly among full-term children. Oscillations within the alpha to beta frequency range play pivotal roles in correlation across cortical regions (Ganzetti & Mantini, 2013). Studies have reported that alpha phase synchronization supports attentional, executive, and contextual functions (Palva & Palva, 2011), while beta oscillations are crucial for heightened sensorimotor transmission, such as visual cue anticipation and processing (Kilavik et al., 2013), as well as for maintaining the status quo and coordinating the integration of visual information related to motion perception (Aissani et al., 2014; De Pasquale et al., 2012). The faster oscillating alpha-beta band synchronization in older full-term infants suggests the emergence of more specialized functional neuronal networks within their visual areas

during motion processing. The transition of oscillation activity from slower theta-band to faster beta and gamma frequencies during radial motion processing in full-term participants signifies developmental progression in neural networks. This developmental pattern may continue into adulthood, as studies in adults implicate increased gamma-band power in visual cortex during motion processing (Hoogenboom et al., 2006; Krishnan et al., 2005; Rice et al., 2013) and in response to moving compared to stationary stimuli (Swettenham et al., 2009). Two nonphase-locked gamma power increases were reported: one initial, rapidly adapting response and one sustained throughout stimulus presentation (Swettenham et al., 2009). The increase in gamma-band neural oscillations is a key signature of information processing in cortical neuronal networks (Muthukumaraswamy & Singh, 2013), reflecting a pattern-matching operation between bottom-up computations and top-down expectancies (Tallon-Baudry, 2003). Therefore, the emergence of synchronized activities in the gamma-band frequency may suggest that 6-year-old children begin to exhibit a more adult-like pattern during the global perception of radial motion, involving the utilization of higher cortical structures and processing information in a more specific and confined manner.

However, unlike the TSEs of full-term infants at 12 months, the TSEs of older preterm infants showed no synchronized oscillatory activities in the alpha-beta range when comparing motion to static. At 6 years of age, although some preterm children exhibited higher synchronizations in the TSEs of comparisons motion to static, most were in the beta-band rather than in the gamma band ranges. The absence of high-frequency oscillatory activities in preterm infants at 12 months and the synchronization in lower frequency at 6 years of age, may indicate slower brain growth and cortical development compared to their full-term peers. These findings are consistent with other studies reporting moderate neurodevelopmental delay in preterm individuals compared to full-term individuals from infancy to childhood (Agyei et al., 2016a; Atkinson & Braddick, 2007; Kapellou et al., 2006; Mewes et al., 2006). One possible contributing factor to this delay could be prematurity disrupting association fibers and synaptic development, which are crucial for fine-tuning cortical growth during late fetal and early extrauterine life (Kapellou et al., 2006). Therefore, preterm birth may hinder the efficient development of the dorsal visual pathway.

The low-frequency desynchronization observed in the TSEs of the visual motion condition contrasted with synchronized activities in the same frequency band and same time range in the TSEs of the static control condition. This suggests that neuronal assemblies may have fired in synchrony when participants perceived a static dot pattern, but this synchronized activity was suppressed under the perception of motion. Given that increased task complexity or heightened attention results in enhanced low-frequency desynchronization (Pfurtscheller et al., 1994), it is plausible that the varying complexities of the presented stimuli, from the relatively simple static dots to the more intricate visual motion, could have contributed to the observed oscillatory differences when perceiving moving versus stationary dots.

The analysis of the localization of the functional connectivity explored the interregional connectivity of dorsal pathway during processing moving and stationary dots in full-term and preterm participants. No connectivity differences were found between moving and stationary dots for either full-term and preterm infants at 4 months or preterm infants at 12 months, while evident connectivity differences between processing motion and static within occipital and parietal areas was found for full-term infants at 12 months and all participants at 6 years of age. This finding is consistent with studies reporting brain

functional correlations originating from the posterior middle temporal complex (MT+) as a result of visual experience (Hidaka et al., 2017; Sani et al., 2010). It also suggests that similar but partially different underlying perceptual processes are involved in processing moving and stationary dots. Localized in the occipital and parietal regions, older full-term infants exhibited one beta-band connectivity difference, while full-term children showed five connectivity differences in the alpha-beta band, and preterm children displayed one connectivity difference in the beta-band when comparing moving and stationary dots. Functional connectivity between visual areas in the occipital and parietal lobes suggests that the connection between these regions subserved visual motion perception, with the lower dorsal stream being more involved during early immature brain development. Notably, only full-term children at 6 years of age displayed interactions with PM source, which marks the beginning of the dorsal pathway. Differences in the number of interactions and the position of brain sources involved support the earlier finding that preterm birth leads to a developmental delay of cortical development and maturation of the dorsal visual stream.

The present study illuminates the divergent developmental trajectories of visual motion perception between full-term and preterm participants from infancy to early childhood. Since this study focused on moderate to very preterm infants, cautioning against generalizing these findings to all premature individuals is necessary. Future investigations could delve deeper into the development of visual motion perception across various premature categories. While full-term participants demonstrated progress in visual motion perception, preterm individuals exhibited poorer sensitivity to optic flow. Although premature children seemed to catch up in some aspects of visual motion perception by early childhood, they may still experience impairments in visual perception. Further follow-up studies could track the evolution of visual motion perception from infancy to adulthood, providing comprehensive insights into specific deficits and compensatory mechanisms over time. The disparities in latency of N2 component, changes in induced oscillatory activity, and brain network connectivity observed in preterm participants compared to their full-term counterparts may signify developmental delays or potentially indicate long-term damages in the dorsal visual stream. Integrating EEG with neuroimaging and neurobiological techniques could unravel the intricate interplay between neurodevelopmental challenges and visual perception. Investigating the specific neural mechanisms underlying impaired dorsal visual stream functioning observed in preterm individuals holds promise for identifying intervention targets and optimizing neurodevelopmental outcomes. Moreover, addressing the challenges posed by infant participants and the limitations of EEG data analysis software is crucial for enhancing the accuracy and reliability of data. Leveraging signal processing methods, machine learning and deep learning, could facilitate stimulation classification and pattern recognition of visual motion perception in infant EEG data with an end-to-end oriented methodology research propelling progression in the field of visual motion perception.

5 Conclusion

The present longitudinal study explored differences in brain electrical activity responses to radial optic flow and random visual motion between full-term and prematurely born individuals from infancy to early childhood, utilizing high-density EEG. Full-term participants increased their sensitivity to optic flow and developed the ability to differentiate between different forms of visual motion towards the end of the first year of life. There was a progression of desynchronized activities from the theta-band to the theta-alpha band and eventually to the alpha-beta range with age, accompanied by more synchronized high-frequency activities in full-term participants. Additionally, greater functional connectivity was observed within occipital and parietal areas in full-term participants, particularly at 6 years of age, suggesting a more adult-like processing of visual motion with a specialized network. In contrast, preterm infants exhibited deficits in distinguishing between different forms of visual motion and showed delayed sensitivity to visual motion, with improvements in N2 component latencies observed when they were 6 years old. They also showed more low-frequency desynchronizations, less high-frequency synchronized oscillatory activity, and diminished functional connectivity in the visual areas during visual motion processing. These findings underscore the divergent developmental trajectories of visual motion perception in preterm individuals compared to their full-term peers. While full-term infants may benefit from neural maturation, preterm individuals often experience neurodevelopmental delays, potentially linked to vulnerabilities in the dorsal visual processing stream. Although premature children showed signs of catching up in some aspects of visual motion perception by early childhood, further research is needed to explore specific deficits and compensatory mechanisms. Crucially, investigating whether these findings signify developmental delays or potential long-term damage in the dorsal visual stream may hold promise in elucidating the intricate interplay between neurodevelopment and visual perception.

References

Agyei, S. B., Holth, M., Van der Weel, F. R., & Van der Meer, A. L. (2015). Longitudinal study of perception of structured optic flow and random visual motion in infants using high-density EEG. *Developmental Science*, *18*(3), 436-451. DOI: 10.1111/desc.12221

Agyei, S. B., Van der Weel, F. R., & Van der Meer, A. L. (2016a). Longitudinal study of preterm and full-term infants: High-density EEG analyses of cortical activity in response to visual motion. *Neuropsychologia*, *84*, 89-104. DOI: 10.1016/j.neuropsychologia.2016.02.001

Agyei, S. B., Van der Weel, F. R., & Van der Meer, A. L. (2016b). Development of visual motion perception for prospective control: brain and behavioral studies in infants. Frontiers in psychology, 7, 172438. DOI: 10.3389/fpsyg.2016.00100

Aissani, C., Martinerie, J., Yahia-Cherif, L., Paradis, A. L., & Lorenceau, J. (2014). Beta, but not gamma, band oscillations index visual form-motion integration. *PLoS One*, *9*(4), e95541. DOI: 10.1371/journal.pone.0095541

Albright, T. D., & Stoner, G. R. (1995). Visual motion perception. *Proceedings of the National Academy of Sciences*, *92*(7), 2433-2440. DOI: 10.1073/pnas.92.7.2433

Atkinson, J., & Braddick, O. (2007). Visual and visuocognitive development in children born very prematurely. *Progress in Brain Research*, *164*, 123-149. DOI: 10.1016/S0079-6123(07)64007-2

Atkinson, J., Braddick, O., Anker, S., Nardini, M., Birtles, D., Rutherford, M. A., ... & Cowan, F. M. (2008). Cortical vision, MRI and developmental outcome in preterm infants. *Archives of Disease in Childhood-Fetal and Neonatal Edition*, *93*(4), F292-F297. DOI: 10.1136/adc.2007.116988

Barzegaran, E., & Knyazeva, M. G. (2017). Functional connectivity analysis in EEG source space: The choice of method. *PLoS One*, *12*(7), e0181105. DOI: 10.1371/journal.pone.0181105

Başar, E., Başar-Eroglu, C., Karakaş, S., & Schürmann, M. (2001). Gamma, alpha, delta, and theta oscillations govern cognitive processes. *International Journal of Psychophysiology*, *39*(2-3), 241-248. DOI: 10.1016/s0167-8760(00)00145-8

Baumberger, B., & Flückiger, M. (2004). The development of distance estimation in optic flow. *Perception*, *33*(9), 1081-1099. DOI: 10.1068/p5063

Beets, I. A. M., Rösler, F., & Fiehler, K. (2010). Nonvisual motor learning improves visual motion perception: Evidence from violating the two-thirds power law. *Journal of Neurophysiology*, *104*(3), 1612-1624. DOI: 10.1152/jn.00974.2009

Bell, M. A., & Fox, N. A. (1996). Crawling experience is related to changes in cortical organization during infancy: Evidence from EEG coherence. *Developmental Psychobiology*, *29*(7), 551-561. DOI: 10.1002/(SICI)1098-2302(199611)29:7<551::AID-DEV1>3.0.CO;2-T

Benassi, M., Bolzani, R., Forsman, L., Ådén, U., Jacobson, L., Giovagnoli, S., & Hellgren, K. (2018). Motion perception and form discrimination in extremely preterm school-aged children. *Child Development*, *89*(6), e494-e506. DOI: 10.1111/cdev.12945

Berg, P., & Scherg, M. (1994). A multiple source approach to the correction of eye artifacts. *Electroencephalography and Clinical Neurophysiology*, *90*(3), 229-241. DOI: 10.1016/0013-4694(94)90094-9

Bertenthal, B. I., Rose, J. L., & Bai, D. L. (1997). Perception–action coupling in the development of visual control of posture. *Journal of experimental psychology: Human Perception and Performance*, *23*(6), 1631. DOI: 10.1037//0096-1523.23.6.1631

Birtles, D. B., Braddick, O. J., Wattam-Bell, J., Wilkinson, A. R., & Atkinson, J. (2007). Orientation and motion-specific visual cortex responses in infants born preterm. *Neuroreport*, *18*(18), 1975-1979.

Blake, R., & Shiffrar, M. (2007). Perception of human motion. *Annu. Rev. Psychol.*, *58*, 47-73. DOI: 10.1097/WNR.0b013e3282f228c8

Bogfjellmo, L. G., Bex, P. J., & Falkenberg, H. K. (2014). The development of global motion discrimination in school aged children. *Journal of Vision*, *14*(2), 19-19. DOI: 10.1167/14.2.19

Bonnier, C. (2008). Evaluation of early stimulation programs for enhancing brain development. *Acta Paediatrica*, *97*(7), 853-858. DOI: 10.1111/j.1651-2227.2008.00834.x

Borge Blystad, J., & Van der Meer, A. L. (2022). Longitudinal study of infants receiving extra motor stimulation, full-term control infants, and infants born preterm: High-density EEG analyses of cortical activity in response to visual motion. *Developmental Psychobiology*, *64*(5), e22276. DOI: 10.1002/dev.22276

Bourgeois, J. P., & Rakic, P. (1993). Changes of synaptic density in the primary visual cortex of the macaque monkey from fetal to adult stage. *Journal of Neuroscience*, *13*(7), 2801-2820. DOI: 10.1523/JNEUROSCI.13-07-02801.1993

Braddick, O., Birtles, D., Wattam-Bell, J., & Atkinson, J. (2005). Motion-and orientation-specific cortical responses in infancy. *Vision Research*, *45*(25-26), 3169-3179. DOI: 10.1016/j.visres.2005.07.021

Brosseau-Lachaine, O., Casanova, C., & Faubert, J. (2008). Infant sensitivity to radial optic flow fields during the first months of life. *Journal of Vision*, *8*(4), 5-5. DOI: 10.1167/8.4.5

Browning, N. A., Grossberg, S., & Mingolla, E. (2009). A neural model of how the brain computes heading from optic flow in realistic scenes. *Cognitive Psychology*, *59*(4), 320-356. DOI: 10.1016/j.cogpsych.2009.07.002

Bruggeman, H., & Warren, W. H. (2010). The direction of walking—but not throwing or kicking—is adapted by optic flow. *Psychological Science*, *21*(7), 1006-1013. DOI: 10.1177/0956797610372635

Budail, R., Contento, G., Locatelli, T., & Comi, G. (1995). Non-invasive multielectrode array for high resolution sampling of scalp-recorded potential fields. *Journal of Medical Engineering & Technology*, *19*(2-3), 52-56. DOI: 10.3109/03091909509030274

Bullmore, E. T., Suckling, J., Overmeyer, S., Rabe-Hesketh, S., Taylor, E., & Brammer, M. J. (1999). Global, voxel, and cluster tests, by theory and permutation, for a difference between two groups of structural MR images of the brain. *IEEE Transactions on Medical Imaging*, *18*(1), 32-42. DOI: 10.1109/42.750253

Buzsaki, G., & Draguhn, A. (2004). Neuronal oscillations in cortical networks. S*cience*, *304*(5679), 1926-1929. DOI: 10.1126/science.1099745

Casey, B. J., Giedd, J. N., & Thomas, K. M. (2000). Structural and functional brain development and its relation to cognitive development. *Biological Psychology*, *54*(1-3), 241-257. DOI: 10.1016/s0301-0511(00)00058-2

Cichocka, M., & Bereś, A. (2018). From fetus to older age: A review of brain metabolic changes across the lifespan. *Ageing Research Reviews*, *46*, 60-73. DOI: 10.1016/j.arr.2018.05.005

Counsell, S. J., & Boardman, J. P. (2005, October). Differential brain growth in the infant born preterm: current knowledge and future developments from brain imaging. In *Seminars in Fetal and Neonatal Medicine* (Vol. 10, No. 5, pp. 403-410). WB Saunders. DOI: 10.1016/j.siny.2005.05.003

Creem, S. H., & Proffitt, D. R. (2001). Defining the cortical visual systems:“what”,“where”, and “how”. *Acta Psychologica*, *107*(1-3), 43-68. DOI: 10.1016/s0001-6918(01)00021-x

David, O., Kilner, J. M., & Friston, K. J. (2006). Mechanisms of evoked and induced responses in MEG/EEG. *Neuroimage*, *31*(4), 1580-1591. DOI: 10.1016/j.neuroimage.2006.02.034

De Pasquale, F., Della Penna, S., Snyder, A. Z., Marzetti, L., Pizzella, V., Romani, G. L., & Corbetta, M. (2012). A cortical core for dynamic integration of functional networks in the resting human brain. *Neuron*, *74*(4), 753-764. DOI: 10.1016/j.neuron.2012.03.031

Domizio, S., Barbante, E., Puglielli, C., Clementini, E., Domizio, R., Sabatino, G. M. D., ... & Sabatino, G. (2005). Excessively high magnetic resonance signal in preterm infants and neuropsychobehavioural follow-up at 2 years. *International Journal of Immunopathology and Pharmacology*, *18*(2), 365-375. DOI: 10.1177/039463200501800218

Duffy, C. J., & Wurtz, R. H. (1991). Sensitivity of MST neurons to optic flow stimuli. I. A continuum of response selectivity to large-field stimuli. *Journal of Neurophysiology*, *65*(6), 1329-1345. DOI: 10.1152/jn.1991.65.6.1329

Elul, R. (1972). The genesis of the EEG. *International Review of Neurobiology*, *15*, 227-272. DOI: 10.1016/s0074-7742(08)60333-5

Orekhova, E. V., Stroganova, T. A., Posikera, I. N., & Elam, M. (2006). EEG theta rhythm in infants and preschool children. *Clinical Neurophysiology*, *117*(5), 1047-1062. DOI: 10.1016/j.clinph.2005.12.027

Ernst, M. D. (2004). Permutation methods: A basis for exact inference. *Statistical Science*, 676-685. DOI: 10.1214/088342304000000396

Fajen, B. R., & Matthis, J. S. (2013). Visual and non-visual contributions to the perception of object motion during self-motion. *PLoS One*, *8*(2), e55446. DOI: 10.1371/journal.pone.0055446

Ferree, T. C., Luu, P., Russell, G. S., & Tucker, D. M. (2001). Scalp electrode impedance, infection risk, and EEG data quality. *Clinical Neurophysiology*, *112*(3), 536-544. DOI: 10.1016/s1388-2457(00)00533-2

Field, A. (2013). *Discovering statistics using IBM SPSS statistics*. sage.

Fielder, A. R., Harper, M. W., Higgins, J. E., Clarke, C. M., & Corrigan, D. (1983). The reliability of the VEP in infancy. *Ophthalmic Paediatrics and Genetics*, *3*(2), 73-82. DOI: 10.3109/13816818309007822

Fields, R. D. (2008). White matter in learning, cognition and psychiatric disorders. *Trends in Neurosciences*, *31*(7), 361-370. DOI: 10.1016/j.tins.2008.04.001

Freunberger, R., Werkle-Bergner, M., Griesmayr, B., Lindenberger, U., & Klimesch, W. (2011). Brain oscillatory correlates of working memory constraints. *Brain Research*, *1375*, 93-102. DOI: 10.1016/j.brainres.2010.12.048

Fujioka, T., Mourad, N., He, C., & Trainor, L. J. (2011). Comparison of artifact correction methods for infant EEG applied to extraction of event-related potential signals. *Clinical Neurophysiology*, *122*(1), 43-51. DOI: 10.1016/j.clinph.2010.04.036

Gallivan, J. P., & Goodale, M. A. (2018). The dorsal “action” pathway. *Handbook of Clinical Neurology*, *151*, 449-466. DOI: 10.1016/B978-0-444-63622-5.00023-1

Ganzetti, M., & Mantini, D. (2013). Functional connectivity and oscillatory neuronal activity in the resting human brain. *Neuroscience*, *240*, 297-309. DOI: 10.1016/j.neuroscience.2013.02.032

Giaschi, D., Zwicker, A., Young, S. A., & Bjornson, B. (2007). The role of cortical area V5/MT+ in speed-tuned directional anisotropies in global motion perception. *Vision Research*, *47*(7), 887-898. DOI: 10.1016/j.visres.2006.12.017

Gibson, J. J. (2014). *The ecological approach to visual perception: classic edition*. Psychology press. DOI: 10.4324/9781315740218

Gilmore, R. O., Baker, T. J., & Grobman, K. H. (2004). Stability in young infants' discrimination of optic flow. *Developmental Psychology*, *40*(2), 259. DOI: 10.1037/0012-1649.40.2.259

Gilmore, R. O., Hou, C., Pettet, M. W., & Norcia, A. M. (2007). Development of cortical responses to optic flow. *Visual Neuroscience*, *24*(6), 845-856. DOI: 10.1017/S0952523807070769

Gilmore, R. O., & Rettke, H. J. (2003). Four-month-olds' discrimination of optic flow patterns depicting different directions of observer motion. *Infancy*, *4*(2), 177-200. DOI: 10.1207/S15327078IN0402_02

Gilmore, R. O., Thomas, A. L., & Fesi, J. (2016). Children's brain responses to optic flow vary by pattern type and motion speed. *PLoS One*, *11*(6), e0157911. DOI: 10.1371/journal.pone.0157911

Gómez-Herrero, G. (2010). Brain connectivity analysis with EEG.

Greenough, W. T., Black, J. E., & Wallace, C. S. (1987). Experience and brain development. *Child Development*, 539-559. DOI: 10.2307/1130197

Grieve, P. G., Emerson, R. G., Fifer, W. P., Isler, J. R., & Stark, R. I. (2003). Spatial correlation of the infant and adult electroencephalogram. *Clinical Neurophysiology*, *114*(9), 1594-1608. DOI: 10.1016/s1388-2457(03)00122-6

Grossberg, S., Mingolla, E., & Pack, C. (1999). A neural model of motion processing and visual navigation by cortical area MST. *Cerebral Cortex*, *9*(8), 878-895. DOI: 10.1093/cercor/9.8.878

Guitton, D., Kearney, R. E., Wereley, N., & Peterson, B. W. (1986). Visual, vestibular and voluntary contributions to human head stabilization. *Experimental Brain Research*, *64*, 59-69. DOI: 10.1007/BF00238201

Gupta, A., Kembhavi, A., & Davis, L. S. (2009). Observing human-object interactions: Using spatial and functional compatibility for recognition. *IEEE Transactions on Pattern Analysis and Machine Intelligence*, *31*(10), 1775-1789. DOI: 10.1109/TPAMI.2009.83

Guzzetta, A., Tinelli, F., Del Viva, M. M., Bancale, A., Arrighi, R., Pascale, R. R., & Cioni, G. (2009). Motion perception in preterm children: Role of prematurity and brain damage. *Neuroreport*, *20*(15), 1339-1343. DOI: 10.1097/WNR.0b013e328330b6f3

Hammarrenger, B., Roy, M. S., Ellemberg, D., Labrosse, M., Orquin, J., Lippe, S., & Lepore, F. (2007). Developmental delay and magnocellular visual pathway function in very-low-birthweight preterm infants. *Developmental Medicine & Child Neurology*, *49*(1), 28-33. DOI: 10.1017/s0012162207000084.x

Hassan, M., Dufor, O., Merlet, I., Berrou, C., & Wendling, F. (2014). EEG source connectivity analysis: from dense array recordings to brain networks. *PloS one*, *9*(8), e105041. DOI: 10.1371/journal.pone.0105041

He, S., Cohen, E. R., & Hu, X. (1998). Close correlation between activity in brain area MT/V5 and the perception of a visual motion aftereffect. *Current Biology*, *8*(22), 1215-1218. DOI: 10.1016/s0960-9822(07)00512-x

Hebart, M. N., & Hesselmann, G. (2012). What visual information is processed in the human dorsal stream?. *Journal of Neuroscience*, *32*(24), 8107-8109. DOI: 10.1523/JNEUROSCI.1462-12.2012

Heinrich, S. P., Renkl, A. E., & Bach, M. (2005). Pattern specificity of human visual motion processing. *Vision Research*, *45*(16), 2137-2143. DOI: 10.1016/j.visres.2005.02.008

Henderson, S. E., Sugden, D., & Barnett, A. L. (1992). Movement assessment battery for children-2. *Research in Developmental Disabilities*. DOI: 10.1037/t55281-000

Hensch, T. K. (2005). Critical period plasticity in local cortical circuits. *Nature Reviews Neuroscience*, *6*(11), 877-888. DOI: 10.1038/nrn1787

Hidaka, S., Higuchi, S., Teramoto, W., & Sugita, Y. (2017). Neural mechanisms underlying sound-induced visual motion perception: An fMRI study. *Acta Psychologica*, *178*, 66-72. DOI: 10.1016/j.actpsy.2017.05.013

Hoechstetter, K., Bornfleth, H., Weckesser, D., Ille, N., Berg, P., & Scherg, M. (2004). BESA source coherence: A new method to study cortical oscillatory coupling. *Brain Topography*, *16*, 233-238. DOI: 10.1023/b:brat.0000032857.55223.5d

Hoogenboom, N., Schoffelen, J. M., Oostenveld, R., Parkes, L. M., & Fries, P. (2006). Localizing human visual gamma-band activity in frequency, time and space. *Neuroimage*, *29*(3), 764-773. DOI: 10.1016/j.neuroimage.2005.08.043

Hudspeth, W. J., & Pribram, K. H. (1992). Psychophysiological indices of cerebral maturation. *International Journal of Psychophysiology*, *12*(1), 19-29. DOI: 10.1016/0167-8760(92)90039-e

Hunnius, S., Geuze, R. H., Zweens, M. J., & Bos, A. F. (2008). Effects of preterm experience on the developing visual system: A longitudinal study of shifts of attention and gaze in early infancy. *Developmental Neuropsychology*, *33*(4), 521-535. DOI: 10.1080/87565640802101508

Ille, N., Berg, P., & Scherg, M. (2002). Artifact correction of the ongoing EEG using spatial filters based on artifact and brain signal topographies. *Journal of Clinical Neurophysiology*, *19*(2), 113-124. DOI: 10.1097/00004691-200203000-00002

Izumi, E., Shirai, N., Kanazawa, S., & K. Yamaguchi, M. (2017). Development of Rigid Motion Perception in Response to Radially Expanding Optic Flow. *Infant and Child Development*, *26*(3), e1989. DOI: 10.1002/icd.1989

Johansson, G. (1975). Visual motion perception. *Scientific American*, *232*(6), 76-89. DOI: 10.1038/scientificamerican0675-76

Johnson, S. P. (2010). How infants learn about the visual world. *Cognitive Science*, *34*(7), 1158-1184. DOI: 10.1111/j.1551-6709.2010.01127.x

Johnson, S. P. (2011). Development of visual perception. *Wiley Interdisciplinary Reviews: Cognitive Science*, *2*(5), 515-528. DOI: 10.1002/wcs.128

Jones, T. A., & Jefferson, S. C. (2011). Reflections of experience-expectant development in repair of the adult damaged brain. *Developmental Psychobiology*, *53*(5), 466-475. DOI: 10.1002/dev.20557

Joshi, M. R., & Falkenberg, H. K. (2015). Development of radial optic flow pattern sensitivity at different speeds. *Vision Research*, *110*, 68-75. DOI: 10.1016/j.visres.2015.03.006

Jouen, F., Lepecq, J. C., Gapenne, O., & Bertenthal, B. I. (2000). Optic flow sensitivity in neonates. *Infant Behavior and Development*, *23*(3-4), 271-284. DOI: 10.1016/S0163-6383(01)00044-3

Kahana, M. J., Seelig, D., & Madsen, J. R. (2001). Theta returns. *Current Opinion in Neurobiology*, *11*(6), 739-744. DOI: 10.1016/s0959-4388(01)00278-1

Kapellou, O., Counsell, S. J., Kennea, N., Dyet, L., Saeed, N., Stark, J., ... & Edwards, A. D. (2006). Abnormal cortical development after premature birth shown by altered allometric scaling of brain growth. *PLoS Medicine*, *3*(8), e265. DOI: 10.1371/journal.pmed.0030265

Kato, T., Nishina, M., Matsushita, K., Hori, E., Mito, T., & Takashima, S. (1997). Neuronal maturation and N-acetyl-L-aspartic acid development in human fetal and child brains. *Brain and Development*, *19*(2), 131-133. DOI: 10.1016/s0387-7604(96)00496-2

Kaufmann, F. (1995). Development of motion perception in early infancy. *European Journal of Pediatrics*, *154*, S48-S53. DOI: 10.1007/BF02191506

Kayed, N. S., & Van der Meer, A. L. (2009). A longitudinal study of prospective control in catching by full-term and preterm infants. *Experimental Brain Research*, *194*, 245-258. DOI: 10.1007/s00221-008-1692-2

Kilavik, B. E., Zaepffel, M., Brovelli, A., MacKay, W. A., & Riehle, A. (2013). The ups and downs of beta oscillations in sensorimotor cortex. *Experimental Neurology*, *245*, 15-26. DOI: 10.1016/j.expneurol.2012.09.014

Kirschen, M. P., Kahana, M. J., Sekuler, R., & Burack, B. (2000). Optic flow helps humans learn to navigate through synthetic environments. *Perception*, *29*(7), 801-818. DOI: 10.1068/p3096

Kirschstein, T., & Köhling, R. (2009). What is the source of the EEG?. *Clinical EEG and Neuroscience*, *40*(3), 146-149. DOI: 10.1177/155005940904000305

Klaver, P., Marcar, V., & Martin, E. (2011). Neurodevelopment of the visual system in typically developing children. *Progress in Brain Research*, *189*, 113-136. DOI: 10.1016/B978-0-444-53884-0.00021-X

Kleinschmidt, A., Thilo, K. V., Büchel, C., Gresty, M. A., Bronstein, A. M., & Frackowiak, R. S. (2002). Neural correlates of visual-motion perception as object-or self-motion. *Neuroimage*, *16*(4), 873-882. DOI: 10.1006/nimg.2002.1181

Klimesch, W., Sauseng, P., & Hanslmayr, S. (2007). EEG alpha oscillations: The inhibition–timing hypothesis. *Brain Research Reviews*, *53*(1), 63-88. DOI: 10.1016/j.brainresrev.2006.06.003

Kobayashi, Y., Yoshino, A., Kawamoto, M., Takahashi, Y., & Nomura, S. (2004). Perception of apparent motion in depth: a high-density electrical mapping study in humans. *Neuroscience Letters*, *354*(2), 115-118. DOI: 10.1016/j.neulet.2003.10.018

Koenderink, J. J. (1986). Optic flow. *Vision Research*, *26*(1), 161-179. DOI: 10.1016/0042-6989(86)90078-7

Kolb, B., & Whishaw, I. Q. (1998). Brain plasticity and behavior. *Annual Review of Psychology*, *49*(1), 43-64. DOI: 10.1146/annurev.psych.49.1.43

Krishnan, A., Kumar, R., Etienne, A., Robinson, A., Kelly, S. K., Behrmann, M., ... & Grover, P. (2018). Challenges and opportunities in instrumentation and use of high-density EEG for underserved regions. In *Innovations and Interdisciplinary Solutions for Underserved Areas: Second*

International Conference, InterSol 2018, Kigali, Rwanda, March 24–25, 2018, Proceedings 2 (pp. 72-82). Springer International Publishing. DOI: 10.1007/978-3-319-98878-8_7

Krishnan, G. P., Skosnik, P. D., Vohs, J. L., Busey, T. A., & O'Donnell, B. F. (2005). Relationship between steady-state and induced gamma activity to motion. *Neuroreport*, *16*(6), 625-630. DOI: 10.1097/00001756-200504250-00022

Kuba, M., & Kubová, Z. (1992). Visual evoked potentials specific for motion onset. *Documenta Ophthalmologica*, *80*, 83-89. DOI: 10.1007/BF00161234

Lalonde-Parsi, M. J., & Lamontagne, A. (2015). Perception of self-motion and regulation of walking speed in young-old adults. *Motor Control*, *19*(3), 191-206. DOI: 10.1123/mc.2014-0010

Lamontagne, A., Fung, J., McFadyen, B. J., & Faubert, J. (2007). Modulation of walking speed by changing optic flow in persons with stroke. *Journal of Neuroengineering and Rehabilitation*, *4*, 1-8. DOI: 10.1186/1743-0003-4-22

Lappe, M., Bremmer, F., & van den Berg, A. V. (1999). Perception of self-motion from visual flow. *Trends in Cognitive Sciences*, *3*(9), 329-336. DOI: 10.1016/s1364-6613(99)01364-9

Layton, O. W., & Fajen, B. R. (2016). A neural model of MST and MT explains perceived object motion during self-motion. *Journal of Neuroscience*, *36*(31), 8093-8102. DOI: 10.1523/JNEUROSCI.4593-15.2016

Leung, M. P., Thompson, B., Black, J., Dai, S., & Alsweiler, J. M. (2018). The effects of preterm birth on visual development. *Clinical and Experimental Optometry*, *101*(1), 4-12. DOI: 10.1111/cxo.12578

Levelt, C. N., & Hübener, M. (2012). Critical-period plasticity in the visual cortex. *Annual Review of Neuroscience*, *35*, 309-330. DOI: 10.1146/annurev-neuro-061010-113813

Loenneker, T., Klaver, P., Bucher, K., Lichtensteiger, J., Imfeld, A., & Martin, E. (2011). Microstructural development: Organizational differences of the fiber architecture between children and adults in dorsal and ventral visual streams. *Human Brain Mapping*, *32*(6), 935-946. DOI: 10.1002/hbm.21080

Luck, S. J. (2014). *An introduction to the event-related potential technique*. MIT press.

Madan, A., Jan, J. E., & Good, W. V. (2005). Visual development in preterm infants. *Developmental Medicine and Child Neurology*, *47*(4), 276-280. DOI: 10.1017/s0012162205000514

Maris, E., & Oostenveld, R. (2007). Nonparametric statistical testing of EEG-and MEG-data. *Journal of Neuroscience Methods*, *164*(1), 177-190. DOI: 10.1016/j.jneumeth.2007.03.024

Mewes, A. U., Hüppi, P. S., Als, H., Rybicki, F. J., Inder, T. E., McAnulty, G. B., ... & Warfield, S. K. (2006). Regional brain development in serial magnetic resonance imaging of low-risk preterm infants. *Pediatrics*, *118*(1), 23-33. DOI: 10.1542/peds.2005-2675

Michel, C. M. (2019). High-resolution EEG. *Handbook of Clinical Neurology*, *160*, 185-201. DOI: 10.1016/B978-0-444-64032-1.00012-6

Milner, D., & Goodale, M. (2006). *The visual brain in action* (Vol. 27). Oup Oxford.

Miskovic, V., Ma, X., Chou, C. A., Fan, M., Owens, M., Sayama, H., & Gibb, B. E. (2015). Developmental changes in spontaneous electrocortical activity and network organization from early to late childhood. *Neuroimage*, *118*, 237-247. DOI: 10.1016/j.neuroimage.2015.06.013

Mohler, B. J., Thompson, W. B., Creem-Regehr, S., Pick, H. L., Warren, W., Rieser, J. J., & Willemsen, P. (2004, August). Visual motion influences locomotion in a treadmill virtual environment. In *Proceedings of the 1st Symposium on Applied Perception in Graphics and Visualization* (pp. 19-22). DOI: 10.1145/1012551.1012554

Molloy, C., Doyle, L. W., Makrides, M., & Anderson, P. J. (2012). Docosahexaenoic acid and visual functioning in preterm infants: a review. *Neuropsychology Review*, *22*, 425-437. DOI: 10.1007/s11065-012-9216-z

Molloy, C. S., Wilson-Ching, M., Anderson, V. A., Roberts, G., Anderson, P. J., & Doyle, L. W. (2013). Visual processing in adolescents born extremely low birth weight and/or extremely preterm. *Pediatrics*, *132*(3), e704-e712. DOI: 10.1542/peds.2013-0040

Morrone, M. C., Tosetti, M., Montanaro, D., Fiorentini, A., Cioni, G., & Burr, D. C. (2000). A cortical area that responds specifically to optic flow, revealed by fMRI. *Nature Neuroscience*, *3*(12), 1322-1328. DOI: 10.1038/81860

Muthukumaraswamy, S. D., & Singh, K. D. (2013). Visual gamma oscillations: The effects of stimulus type, visual field coverage and stimulus motion on MEG and EEG recordings. *Neuroimage*, *69*, 223-230. DOI: 10.1016/j.neuroimage.2012.12.038

Newsome, W. T., & Pare, E. B. (1988). A selective impairment of motion perception following lesions of the middle temporal visual area (MT). *Journal of Neuroscience*, *8*(6), 2201-2211. DOI: 10.1523/JNEUROSCI.08-06-02201.1988

Niehorster, D. C. (2021). Optic flow: A history. *I-Perception*, *12*(6), 20416695211055766. DOI: 10.1177/20416695211055766

Niell, C. M., & Stryker, M. P. (2010). Modulation of visual responses by behavioral state in mouse visual cortex. *Neuron*, *65*(4), 472-479. DOI: 10.1016/j.neuron.2010.01.033

Odom, J. V., Bach, M., Barber, C., Brigell, M., Marmor, M. F., Tormene, A. P., ... & Vaegan. (2004). Visual evoked potentials standard (2004). *Documenta Ophthalmologica*, *108*, 115-123. DOI: 10.1023/b:doop.0000036790.67234.22

Ohuma, E. O., Moller, A. B., Bradley, E., Chakwera, S., Hussain-Alkhateeb, L., Lewin, A., ... & Moran, A. C. (2023). National, regional, and global estimates of preterm birth in 2020, with trends from 2010: A systematic analysis. *The Lancet*, *402*(10409), 1261-1271. DOI: 10.1016/S0140-6736(23)00878-4

Ortibus, E. L., De Cock, P. P., & Lagae, L. G. (2011). Visual perception in preterm children: What are we currently measuring?. *Pediatric Neurology*, *45*(1), 1-10. DOI: 10.1016/j.pediatrneurol.2011.02.008

O'Connor, D. L., Hall, R., Adamkin, D., Auestad, N., Castillo, M., Connor, W. E., ... & Ross Preterm Lipid Studya. (2001). Growth and development in preterm infants fed long-chain polyunsaturated fatty acids: A prospective, randomized controlled trial. *Pediatrics*, *108*(2), 359-371. DOI: 10.1542/peds.108.2.359

Palva, S., & Palva, J. M. (2011). Functional roles of alpha-band phase synchronization in local and large-scale cortical networks. *Frontiers in Psychology*, *2*, 10776. DOI: 10.3389/fpsyg.2011.00204

Parrish, E. E., Giaschi, D. E., Boden, C., & Dougherty, R. (2005). The maturation of form and motion perception in school age children. *Vision Research*, *45*(7), 827-837. DOI: 10.1016/j.visres.2004.10.005

Paus, T., Collins, D. L., Evans, A. C., Leonard, G., Pike, B., & Zijdenbos, A. (2001). Maturation of white matter in the human brain: a review of magnetic resonance studies. *Brain Research Bulletin*, *54*(3), 255-266. DOI: 10.1016/s0361-9230(00)00434-2

Pel, J. J., Dudink, J., Vonk, M., Plaisier, A., Reiss, I. K., & Van der Steen, J. (2016). Early identification of cerebral visual impairments in infants born extremely preterm. *Developmental Medicine & Child Neurology*, *58*(10), 1030-1035. DOI: 10.1111/dmcn.13115

Perez-Roche, T., Altemir, I., Giménez, G., Prieto, E., González, I., Peña-Segura, J. L., ... & Pueyo, V. (2016). Effect of prematurity and low birth weight in visual abilities and school performance. *Research in Developmental Disabilities*, *59*, 451-457. DOI: 10.1016/j.ridd.2016.10.002

Pfurtscheller, G. (2001). Functional brain imaging based on ERD/ERS. *Vision Research*, *41*(10-11), 1257-1260. DOI: 10.1016/s0042-6989(00)00235-2

Pfurtscheller, G., & Da Silva, F. L. (1999). Event-related EEG/MEG synchronization and desynchronization: basic principles. *Clinical Neurophysiology*, *110*(11), 1842-1857. DOI: 10.1016/s1388-2457(99)00141-8

Pfurtscheller, G., Neuper, C., & Mohl, W. (1994). Event-related desynchronization (ERD) during visual processing. *International Journal of Psychophysiology*, *16*(2-3), 147-153. DOI: 10.1016/0167-8760(89)90041-x

Picton, T. W., Bentin, S., Berg, P., Donchin, E., Hillyard, S. A., Johnson, R., ... & Taylor, M. J. (2000). Guidelines for using human event-related potentials to study cognition: recording standards and publication criteria. *Psychophysiology*, *37*(2), 127-152. DOI: 10.1111/1469-8986.3720127

Probst, T., Plendl, H., Paulus, W., Wist, E. R., & Scherg, M. (1993). Identification of the visual motion area (area V5) in the human brain by dipole source analysis. *Experimental Brain Research*, *93*, 345-351. DOI: 10.1007/BF00228404

Rasulo, S., Vilhelmsen, K., Van der Weel, F. R., & Van der Meer, A. L. (2021). Development of motion speed perception from infancy to early adulthood: A high-density EEG study of simulated forward motion through optic flow. *Experimental Brain Research*, *239*(10), 3143-3154. DOI: 10.1007/s00221-021-06195-5

Raudies, F., Gilmore, R. O., Kretch, K. S., Franchak, J. M., & Adolph, K. E. (2012, November). Understanding the development of motion processing by characterizing optic flow experienced by infants and their mothers. In *2012 IEEE International Conference on Development and Learning and Epigenetic Robotics (ICDL)* (pp. 1-6). IEEE. DOI: 10.1109/DevLrn.2012.6400584

Regan, D. (1989). Evoked potentials and evoked magnetic fields in science and medicine. *Human Brain Electrophysiology*, 59-61.

Rice, J. K., Rorden, C., Little, J. S., & Parra, L. C. (2013). Subject position affects EEG magnitudes. *NeuroImage*, *64*, 476-484. DOI: 10.1016/j.neuroimage.2012.09.041

Rinaldi, N. M., Polastri, P. F., & Barela, J. A. (2009). Age-related changes in postural control sensory reweighting. *Neuroscience Letters*, *467*(3), 225-229. DOI: 10.1016/j.neulet.2009.10.042

Rosander, K., Nyström, P., Gredebäck, G., & von Hofsten, C. (2007). Cortical processing of visual motion in young infants. *Vision Research*, *47*(12), 1614-1623. DOI: 10.1016/j.visres.2007.03.004

Rosenberg, J. R., Amjad, A. M., Breeze, P., Brillinger, D. R., & Halliday, D. M. (1989). The Fourier approach to the identification of functional coupling between neuronal spike trains. *Progress in Biophysics and Molecular Biology*, *53*(1), 1-31. DOI: 10.1016/0079-6107(89)90004-7

Saleem, A. B., Ayaz, A., Jeffery, K. J., Harris, K. D., & Carandini, M. (2013). Integration of visual motion and locomotion in mouse visual cortex. *Nature Neuroscience*, *16*(12), 1864-1869. DOI: 10.1038/nn.3567

Sani, L., Ricciardi, E., Gentili, C., Vanello, N., Haxby, J. V., & Pietrini, P. (2010). Effects of visual experience on the human MT+ functional connectivity networks: an fMRI study of motion perception in sighted and congenitally blind individuals. *Frontiers in Systems Neuroscience*, *4*, 159. DOI: 10.3389/fnsys.2010.00159

Scherg, M., & Berg, P. (1991). Use of prior knowledge in brain electromagnetic source analysis. *Brain Topography*, *4*, 143-150. DOI: 10.1007/BF01132771

Scherg, M., Ille, N., Bornfleth, H., & Berg, P. (2002). Advanced Tools for Digital EEG review:: virtual source montages, whole-head mapping, correlation, and phase analysis. *Journal of Clinical Neurophysiology*, *19*(2), 91-112. DOI: 10.1097/00004691-200203000-00001

Schoffelen, J. M., & Gross, J. (2009). Source connectivity analysis with MEG and EEG. *Human Brain Mapping*, *30*(6), 1857-1865. DOI: 10.1002/hbm.20745

Shao, S. Y., Shen, K. Q., Ong, C. J., & Wilder-Smith, E. P. (2008). Automatic EEG artifact removal: a weighted support vector machine approach with error correction. *IEEE Transactions on Biomedical Engineering*, *56*(2), 336-344. DOI: 10.1109/TBME.2008.2005969

Shirai, N., & Imura, T. (2014). Looking away before moving forward: Changes in optic-flow perception precede locomotor development. *Psychological Science*, *25*(2), 485-493. DOI: 10.1177/0956797613510723

Shirai, N., Kanazawa, S., & Yamaguchi, M. K. (2008). Sensitivity to rotational motion in early infancy. *Experimental Brain Research*, *190*, 201-206. DOI: 10.1007/s00221-008-1461-2

Shirai, N., & Yamaguchi, M. K. (2010). How do infants utilize radial optic flow for their motor actions?: A review of behavioral and neural studies. *Japanese Psychological Research*, *52*(2), 78-90. DOI: 10.1111/j.1468-5884.2010.00426.x

Singer, W. (1993). Synchronization of cortical activity and its putative role in information processing and learning. *Annual Review of Physiology*, *55*(1), 349-374. DOI: 10.1146/annurev.ph.55.030193.002025

Smith, A. T., Wall, M. B., Williams, A. L., & Singh, K. D. (2006). Sensitivity to optic flow in human cortical areas MT and MST. *European Journal of Neuroscience*, *23*(2), 561-569. DOI: 10.1111/j.1460-9568.2005.04526.x

Srinivasan, R., Winter, W. R., Ding, J., & Nunez, P. L. (2007). EEG and MEG coherence: measures of functional connectivity at distinct spatial scales of neocortical dynamics. *Journal of Neuroscience Methods*, *166*(1), 41-52. DOI: 10.1016/j.jneumeth.2007.06.026

Sripada, K., Løhaugen, G. C., Eikenes, L., Bjørlykke, K. M., Håberg, A. K., Skranes, J., & Rimol, L. M. (2015). Visual–motor deficits relate to altered gray and white matter in young adults born preterm with very low birth weight. *Neuroimage*, *109*, 493-504. DOI: 10.1016/j.neuroimage.2015.01.019

Stroganova, T. A., Orekhova, E. V., & Posikera, I. N. (1999). EEG alpha rhythm in infants. *Clinical Neurophysiology*, *110*(6), 997-1012. DOI: 10.1016/s1388-2457(98)00009-1

Strong, S. L., Silson, E. H., Gouws, A. D., Morland, A. B., & McKeefry, D. J. (2017). A direct demonstration of functional differences between subdivisions of human V5/MT+. *Cerebral Cortex*, *27*(1), 1-10. DOI: 10.1093/cercor/bhw362

Swettenham, J. B., Muthukumaraswamy, S. D., & Singh, K. D. (2009). Spectral properties of induced and evoked gamma oscillations in human early visual cortex to moving and stationary stimuli. *Journal of Neurophysiology*, *102*(2), 1241-1253. DOI: 10.1152/jn.91044.2008

Takesian, A. E., & Hensch, T. K. (2013). Balancing plasticity/stability across brain development. *Progress in Brain Research*, *207*, 3-34. DOI: 10.1016/B978-0-444-63327-9.00001-1

Talairach, P. J. (1988). Co-planar stereotaxic atlas of the human brain. *(No Title)*.

Tallon-Baudry, C. (2003). Oscillatory synchrony and human visual cognition. *Journal of Physiology-Paris*, *97*(2-3), 355-363. DOI: 10.1016/j.jphysparis.2003.09.009

Taylor, N. M., Jakobson, L. S., Maurer, D., & Lewis, T. L. (2009). Differential vulnerability of global motion, global form, and biological motion processing in full-term and preterm children. *Neuropsychologia*, *47*(13), 2766-2778. DOI: 10.1016/j.neuropsychologia.2009.06.001

Thierry, G. (2005). The use of event-related potentials in the study of early cognitive development. *Infant and Child Development*, *14*(1), 85-94. DOI: 10.1002/icd.353

Tootell, R. B., Reppas, J. B., Kwong, K. K., Malach, R., Born, R. T., Brady, T. J., ... & Belliveau, J. W. (1995). Functional analysis of human MT and related visual cortical areas using magnetic resonance imaging. *Journal of Neuroscience*, *15*(4), 3215-3230. DOI: 10.1523/JNEUROSCI.15-04-03215.1995

Vaina, L. M., & Rushton, S. K. (2000). What neurological patients tell us about the use of optic flow. *International Review of Neurobiology*, *44*, 293-313. DOI: 10.1016/s0074-7742(08)60747-3

Van der Meer, A. L., Fallet, G., & Van der Weel, F. R. (2008). Perception of structured optic flow and random visual motion in infants and adults: a high-density EEG study. *Experimental Brain Research*, *186*, 493-502. DOI: 10.1007/s00221-007-1251-2

Van der Weel, F. R., & Van der Meer, A. L. (2009). Seeing it coming: Infants' brain responses to looming danger. *Naturwissenschaften*, *96*, 1385-1391. DOI: 10.1007/s00114-009-0585-y

Vilhelmsen, K., Agyei, S. B., Van der Weel, F. R., & Van der Meer, A. L. (2019). A high-density EEG study of differentiation between two speeds and directions of simulated optic flow in adults and infants. *Psychophysiology*, *56*(1), e13281. DOI: 10.1111/psyp.13281

Vilhelmsen, K., Van der Weel, F. R., & Van der Meer, A. L. (2015). A high-density EEG study of differences between three high speeds of simulated forward motion from optic flow in adult participants. *Frontiers in Systems Neuroscience*, *9*, 146. DOI: 10.3389/fnsys.2015.00146

Warren Jr, W. H., & Hannon, D. J. (1988). Direction of self-motion is perceived from optical flow. *Nature*, *336*(6195), 162-163. DOI: 10.1038/336162a0

Warren, W. H., Kay, B. A., Zosh, W. D., Duchon, A. P., & Sahuc, S. (2001). Optic flow is used to control human walking. *Nature Neuroscience*, *4*(2), 213-216. DOI: 10.1038/84054

Wilkie, R. M., & Wann, J. P. (2003). Eye-movements aid the control of locomotion. *Journal of Vision*, *3*(11), 3-3. DOI: 10.1167/3.11.3

Xie, W., Toll, R. T., & Nelson, C. A. (2022). EEG functional connectivity analysis in the source space. *Developmental Cognitive Neuroscience*, *56*, 101119. DOI: 10.1016/j.dcn.2022.101119

Yonas, A. (1981). Infants' responses to optical information for collision. *Development of Perception: Psychobiological Perspectives*, 313-334. DOI: 10.1016/B978-0-12-065302-7.50021-8

Zeki, S., Watson, J. D., Lueck, C. J., Friston, K. J., Kennard, C., & Frackowiak, R. S. (1991). A direct demonstration of functional specialization in human visual cortex. *Journal of Neuroscience*, *11*(3), 641-649. DOI: 10.1523/JNEUROSCI.11-03-00641.1991

Zemel, R. S., & Sejnowski, T. J. (1998). A model for encoding multiple object motions and self-motion in area MST of primate visual cortex. *Journal of Neuroscience*, *18*(1), 531-547. DOI: 10.1523/JNEUROSCI.18-01-00531.1998

Appendices

Appendix 1:

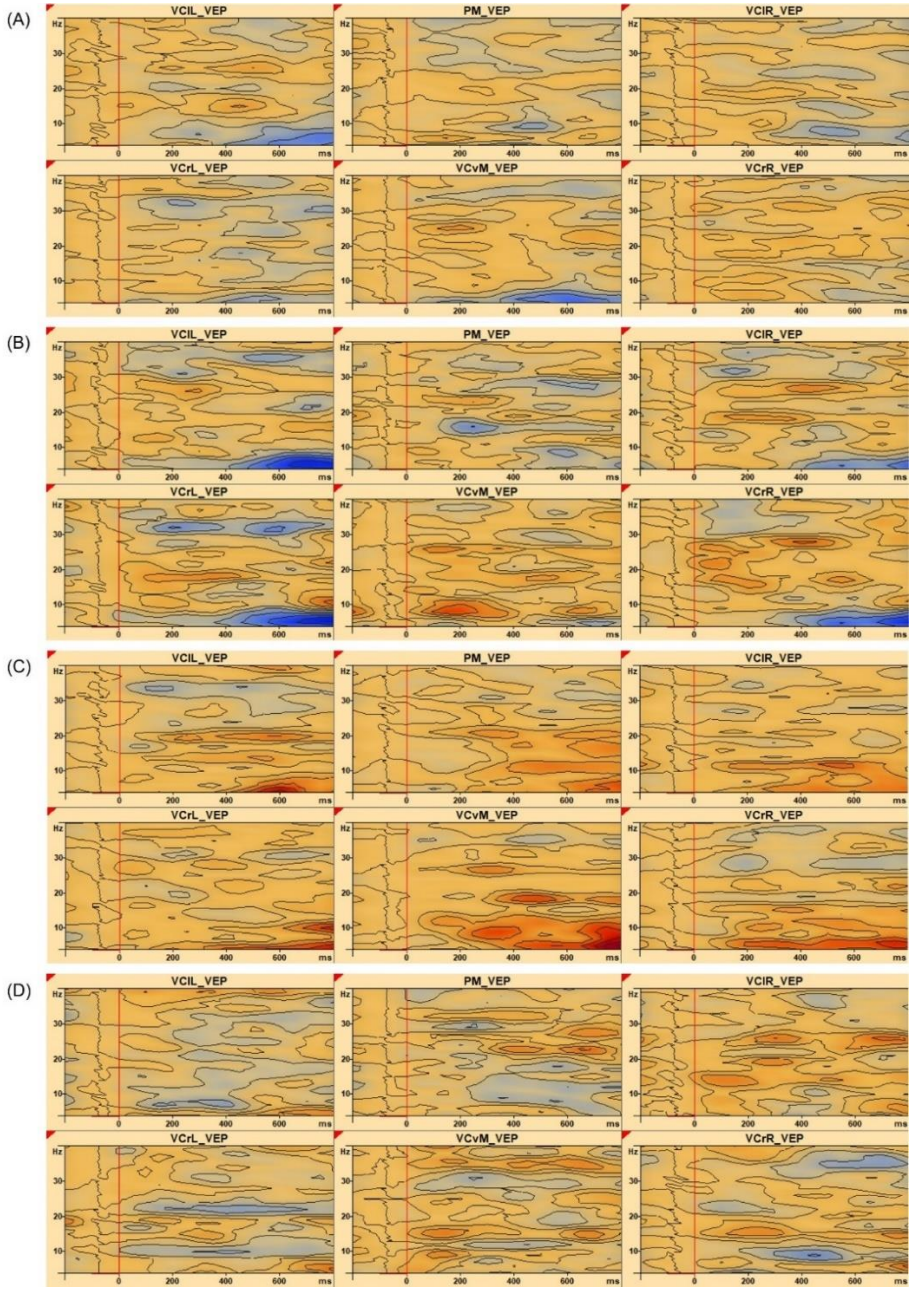

TSE plots of visual motion condition (A, B) and static control condition (C, D) across brain regions of interest (VClL, VCrL, PM, VCvM, VCrR, and VClR) at 4 months in full-term infant I (A, C) and preterm infant M (B, D). In the TSE plots, decreased spectral amplitude (induced desynchronized activity) and increased spectral amplitude (induced synchronized activity) are shown in blue and red contours, respectively. Induced theta-band desynchronized activities were predominantly observed in the visual areas of interest in the TSEs of the visual motion condition (A, B), while synchronized activities in the same frequency band were evident in the TSE of the static control condition (C, D). Stimulus onset is indicated with a red vertical line at 0ms with epoch set from -200ms to 800ms and baseline at -100ms to 0ms.

Appendix 2:

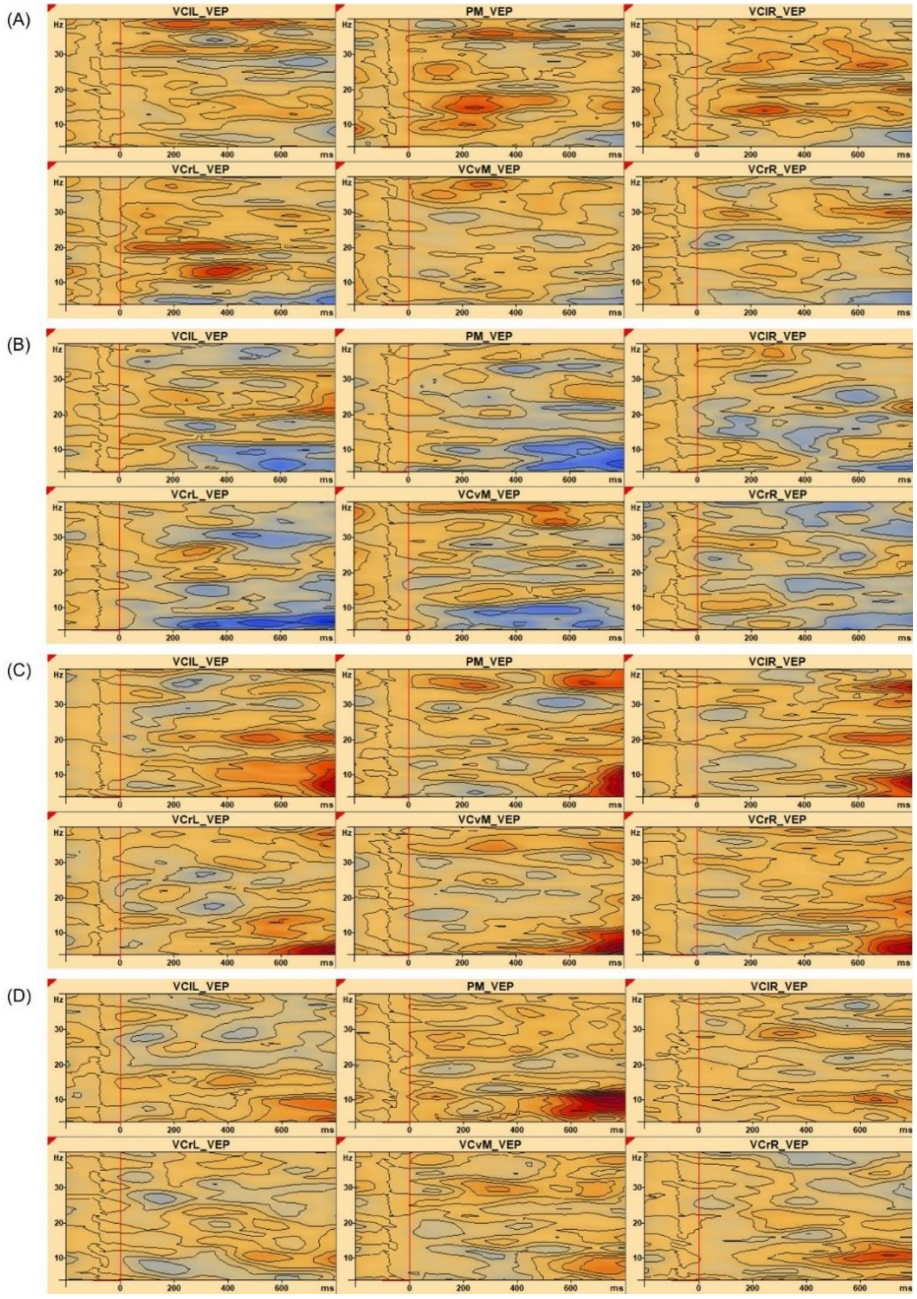

TSE plots of visual motion condition (A, B) and static control condition (C, D) across brain regions of interest (VClL, VCrL, PM, VCvM, VCrR, and VClR) at 12 months in full-term infant H (A, C) and preterm infant K (B, D). In the TSE plots, decreased spectral amplitude (induced desynchronized activity) and increased spectral amplitude (induced synchronized activity) are shown in blue and red contours, respectively. Induced theta-band desynchronized activities were predominantly observed in the visual areas of interest in the TSEs of the visual motion condition (A, B), while synchronized activities in the same frequency band were evident in the TSE of the static control condition (C, D). Full-term infants displayed higher synchronized activity in the late alpha and early beta ranges in the TSEs of the visual motion condition (A), occurring as the desynchronized activity within the same frequency range in the static control condition (C), while preterm infants exhibited desynchronized activity in the alpha-beta band in the visual motion condition (B). Stimulus onset is indicated with a red vertical line at 0ms with epoch set from -200ms to 800ms and baseline at -100ms to 0ms.

Appendix 3:

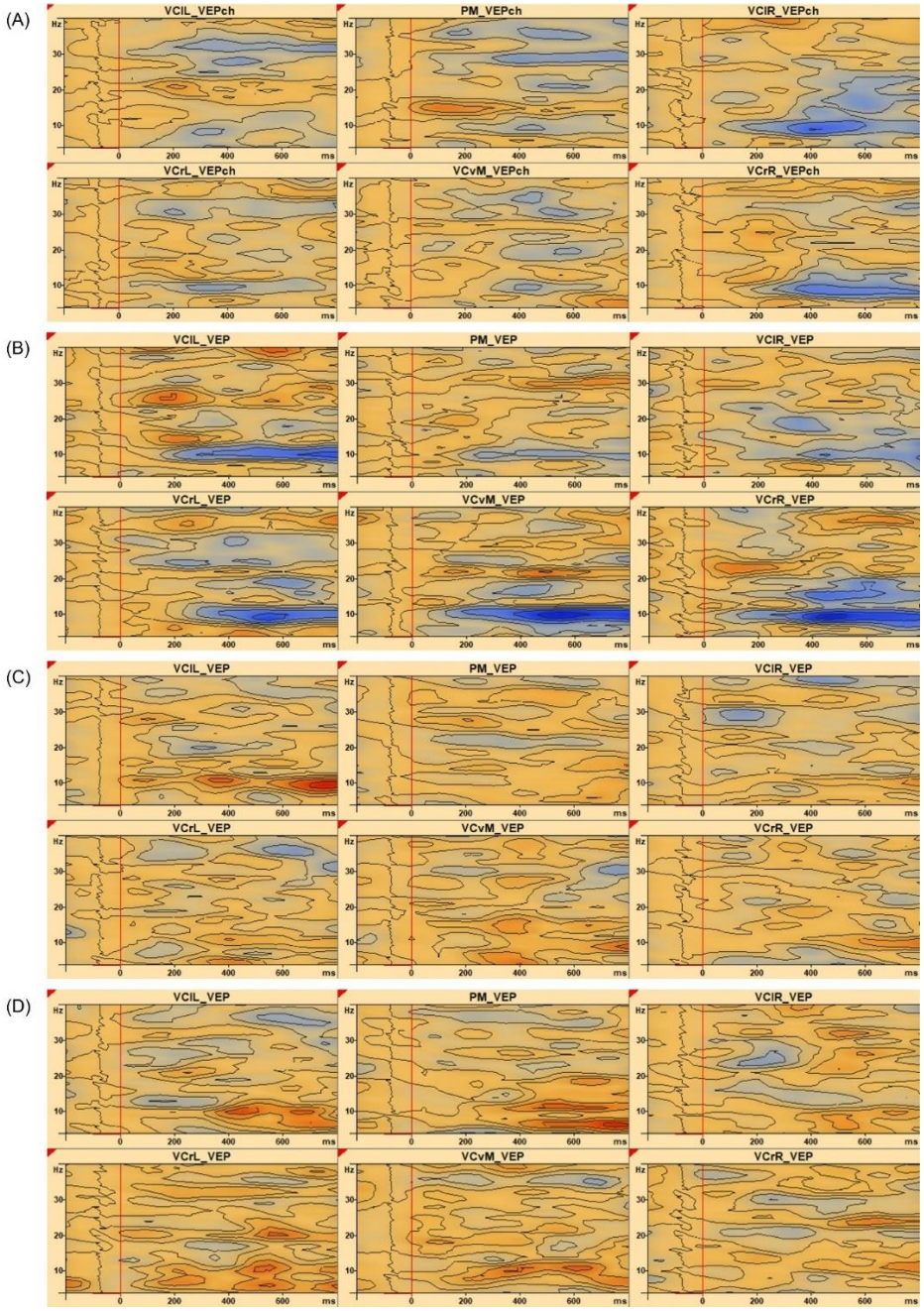

TSE plots of visual motion condition (A, B) and static control condition (C, D) across brain regions of interest (VCIL, VCrL, PM, VCvM, VCrR, and VCIR) at 6 years of age in full-term child H (A, C) and preterm child M (B, D). In the TSE plots, decreased spectral amplitude (induced desynchronized activity) and increased spectral amplitude (induced synchronized activity) are shown in blue and red contours, respectively. Induced desynchronized activities in the late alpha and early beta ranges were predominantly observed in the visual areas of interest in the TSEs of the visual motion condition (A, B), while synchronized activities in the same frequency band were evident in the TSE of the static control condition (C, D). These activities were more pronounced in preterm children than in full-term children. Stimulus onset is indicated with a red vertical line at 0ms with epoch set from -200ms to 800ms and baseline at -100ms to 0ms.

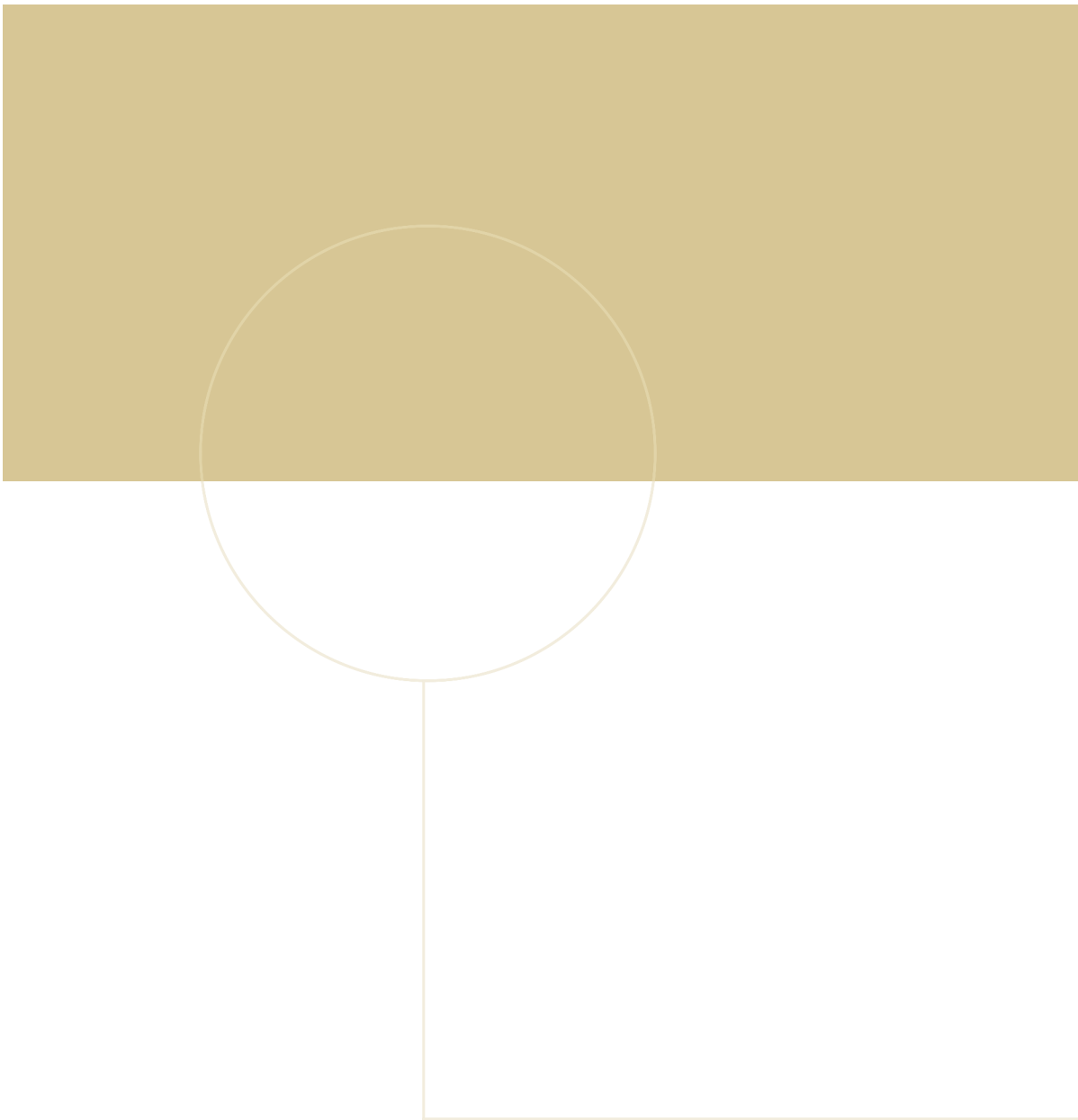

NTNU

Norwegian University of
Science and Technology